

Synthesis and reactivity of PC(sp³)P-pincer iridium complexes bearing diborylmethyl anion

Masamichi Kishino, Satoko Takaoka, Yuki Shibutani, Shuhei Kusumoto,* and Kyoko Nozaki*

*Department of Chemistry and Biotechnology, Graduate School of Engineering,
The University of Tokyo, 7-3-1 Hongo, Bunkyo-ku, Tokyo 113-8656, Japan.*

Contents:	page
I. Experimental Section	
I-I. General	S2
I-II. Preparation & NMR Data of the Novel Compounds	S3
I-III. Dehydrogenation of Cyclooctane	S27
II. IR Spectra of the Novel Compounds	S28
III. Detail for the X-ray Crystallographic Analyses	S32
IV. Methods and Discussions for Theoretical Calculations	
IV-I. NBO and MO Analysis of Complex 7_{Me}	S36
IV-II. Calculated Molecular Orbitals of Complexes 8_{Me} and C_{Me}	S38
IV-III. Deuterium Incorporation at the α-Position	S39
V. References	S41

I. Experimental Section

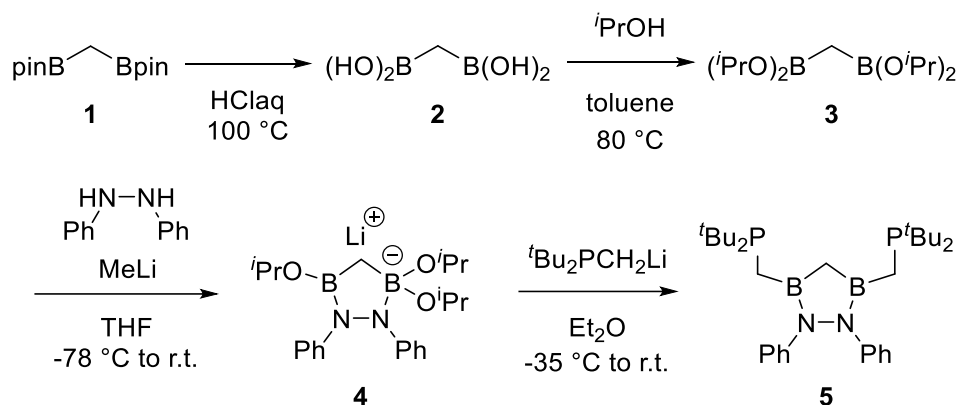
I-I. General

Manipulation: All reactions were carried out using a standard glovebox or Schlenk techniques under nitrogen or argon gas purified by passing through Nikka Seiko dry column DC-L4 (NIKKA SEIKO Co., Ltd.).

Instrumentation: Nuclear magnetic resonance (NMR) spectra were recorded on BRUKER Ascend500 (^1H : 500 MHz, ^{13}C : 126 MHz, ^{11}B : 160 MHz, ^{31}P : 202 MHz with digital resolution of 0.305, 0.908, 0.98, 2.49 Hz, respectively), or JEOL ECS400 (^1H : 400 MHz, ^2H : 61 MHz with digital resolution of 0.11, 0.05 Hz, respectively) at ambient temperature unless otherwise noted. Chemical shifts are reported in ppm relative to the residual protiated solvent for ^1H (benzene- d_6 (C_6D_6) 7.16 ppm, tetrahydrofuran- d_8 (THF- d_8) 3.58 ppm), the deuterated solvent for ^{13}C (C_6D_6 128.06 ppm, THF- d_8 67.21 ppm) and ^2H (C_6D_6 7.16 ppm), external $(\text{C}_2\text{H}_5)_2\text{O}\cdot\text{BF}_3$ standard for ^{11}B nuclei, and external 85% H_3PO_4 standard for ^{31}P nuclei. Mass spectra (MS) were taken with an electron spray ionization time-of-flight (ESI-TOF) method on a JEOL JMS-T100LP AccuTOF LC-plus mass spectrometer. Infrared (IR) spectra were recorded on a Shimadzu FTIR-8400 or a JASCO FTIR-6600 equipped with an attenuated total reflection (ATR) system. X-ray crystallographic analyses were performed on a Rigaku Varimax dual with Saturn diffractometer or with hybrid photon counting detector. Elemental analyses were performed by Microanalytical Laboratory of Department of Chemistry, Graduate School of Science, the University of Tokyo.

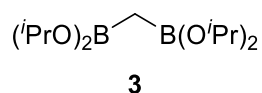
Materials: Anhydrous diethyl ether, hexane, tetrahydrofuran (THF), and toluene were purchased from Kanto Chemical Co., Inc. (Kanto) and purified by the method of Pangborn *et al.*¹ The following solvents and reagents were purchased and used as received: *n*-pentane, dehydrated -super- (FUJIFILM Wako Pure Chemical Co., Ltd. (Wako)), benzene, dehydrated -super- (Wako), 2-propanol (Wako), hydrazobenzene (Tokyo Chemical Industry Co., Ltd. (TCI)), methyllithium solution in diethyl ether (Br free) (Kanto). Sodium hydride (60%, dispersion in paraffin liquid) was purchased from TCI and used after paraffin liquid was removed with hexane. C_6D_6 (Aldrich) was dehydrated with preactivated molecular sieves 3A. THF- d_8 (Aldrich) was dehydrated with NaK. Carbon monoxide gas (Taiyo Nippon Sanso JFP Co.) was purified by passing through a dry column (DC-HDF300-A3, Nikka Seiko Co., Ltd.). The following reagents were prepared according to the literature procedures: methylenebis(boronic acid) (**2**),² di-*tert*-butylphosphinomethylithium,³ chlorobis(cyclooctene)iridium dimer,⁴ bis(trimethylsilyl)methylithium.⁵

I-II. Preparation & NMR Data of the Novel Compounds



Scheme S1. The entire procedure for the synthesis of the ligand precursor **5**.

B,B'-methylenebis-[B,B',B',-tetra-(2-propyl) ester boronic acid] (**3**)



To a solution of methylenebis(boronic acid) (**2**) (7.35 g, 70.9 mmol) in toluene (150 mL), 2-propanol (45 mL, 585 mmol) and the preactivated molecular sieve 3A were added. The mixture was stirred at 80 °C for 5 days. After removal of the molecular sieve by filtration, the solvent was removed under reduced pressure. The desired compound **3** was obtained as colourless or pale-yellow oil (12.85 g, 67% yield).

^1H NMR (500 MHz, C_6D_6) δ : 4.61 (sept, $J = 6.1$ Hz, 4H), 1.19 (d, $J = 6.1$ Hz, 24H), 0.55 (s, 2H); ^{13}C NMR (126 MHz, C_6D_6) δ : 65.5 (s, 4C), 24.8 (s, 8C), 1.4 (br, 1C); $^{11}\text{B}\{^1\text{H}\}$ NMR (160 MHz, C_6D_6) δ : 30.6; HRMS (ESI) m/z calcd for $\text{C}_{13}\text{H}_{30}\text{B}_2\text{NaO}_4$ [$\text{M}+\text{Na}$] $^+$ 295.2222, found 295.2210; IR (neat) cm^{-1} 2972, 1468, 1370.

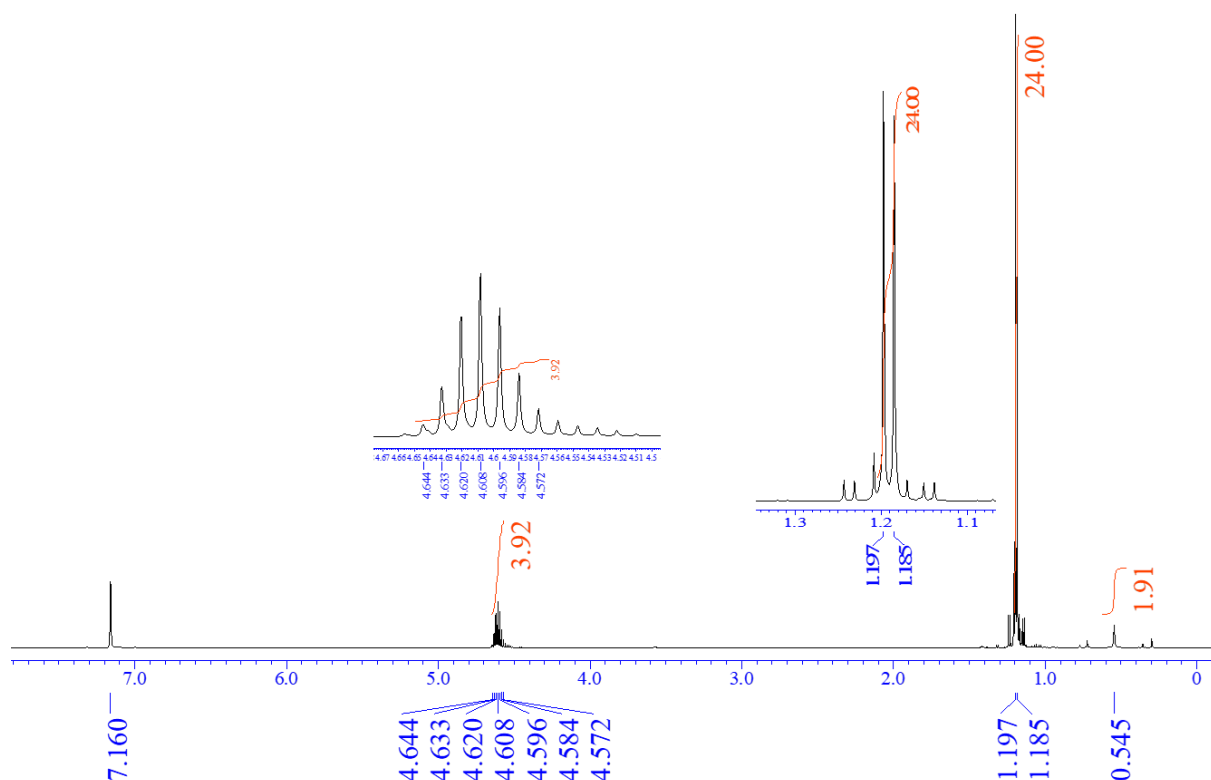


Figure S1. ^1H NMR spectrum of compound **3** (C_6D_6 , 500 MHz).

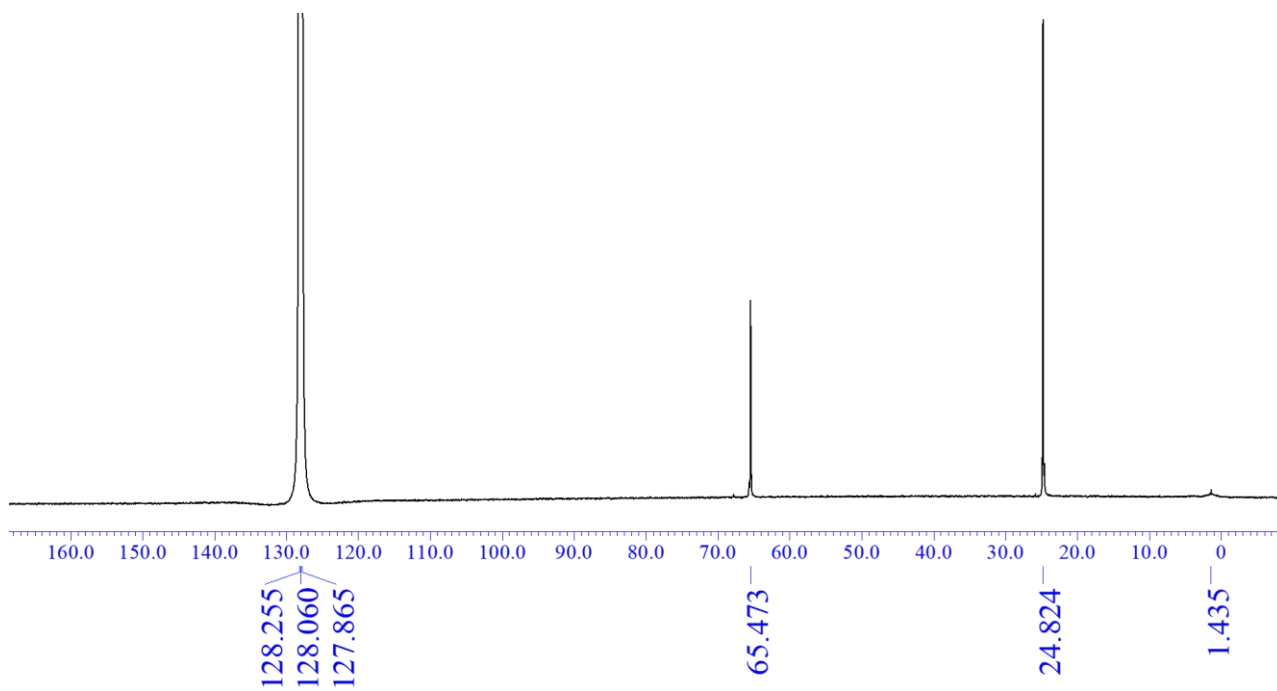


Figure S2. ^{13}C NMR spectrum of compound **3** (C_6D_6 , 126 MHz).

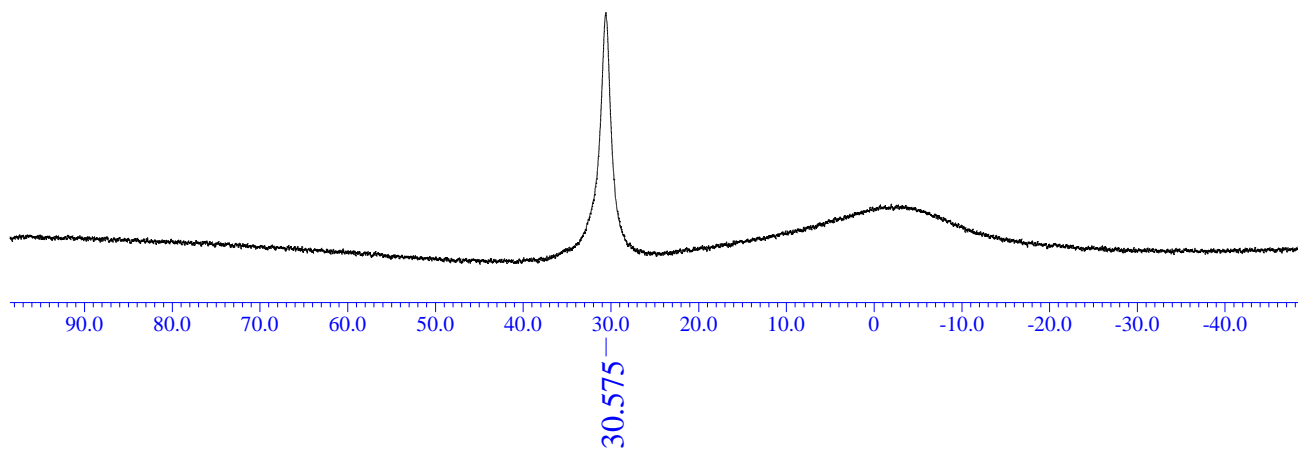
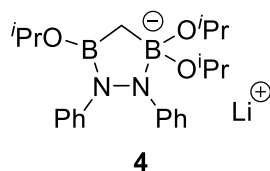


Figure S3. $^{11}\text{B}\{^1\text{H}\}$ NMR spectrum of compound **3** (C_6D_6 , 160 MHz).

Lithium 1,2-diphenyl-3-(2-propoxy)-4,4-di(2-propoxy)-1,2-diaza-3,5-diborolanate (**4**)



To a solution of hydrazobenzene (3.39 g, 18.4 mmol) in THF (80 mL), methyllithium solution in diethyl ether (Br free) (1.04 M, 36 mL, 37.4 mmol) was added dropwise at -78 °C. After the mixture was stirred at -78 °C for 3 h, compound **3** was added at -78 °C. The mixture was stirred at -78 °C for 30 min, then at room temperature for 12 h. The solvent was removed under reduced pressure. The residue was recrystallized from toluene at -35 °C to afford the desired compound **4** as colourless crystals. The obtained crystals were washed well with hexane (6.78 g, 92% yield). Although **4** was obtained as crystal in almost pure form, ¹H and ¹³C NMR spectra always show complicated mixture probably due to the dynamic dissociation and recombination of isopropoxy groups, see Figure S4 and S5. The obtained solid was used in the next step to synthesize **5**.

¹H NMR (500 MHz, THF-*d*₈) see Figure S4; ¹³C NMR (126 MHz, THF-*d*₈) see Figure S5; ¹¹B{¹H} NMR (160 MHz, THF-*d*₈); 38.5, 8.50; HRMS (ESI) *m/z* calcd for C₂₂H₃₄B₂LiN₂O₃ [M+H]⁺ 403.2910, found 403.2896; IR (neat) cm⁻¹ 3327, 2962, 2922, 2872, 1589, 1485.

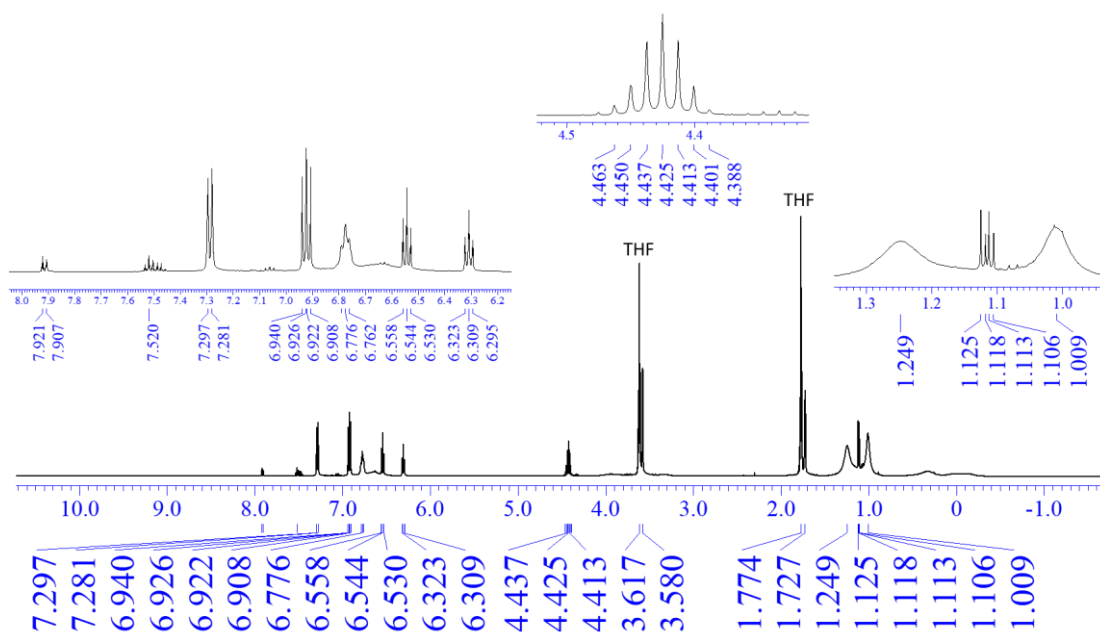


Figure S4. ¹H NMR spectrum of compound **4** (THF-*d*₈, 500 MHz).

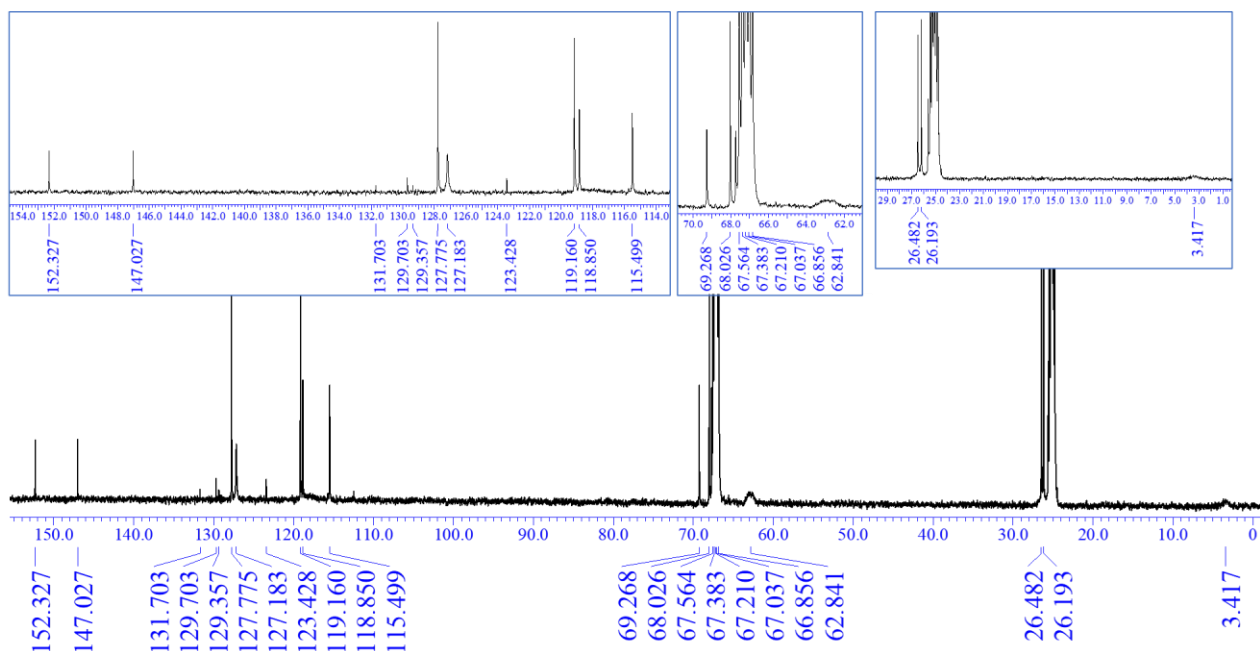


Figure S5. ^{13}C NMR spectrum of compound **4** ($\text{THF-}d_8$, 126 MHz).

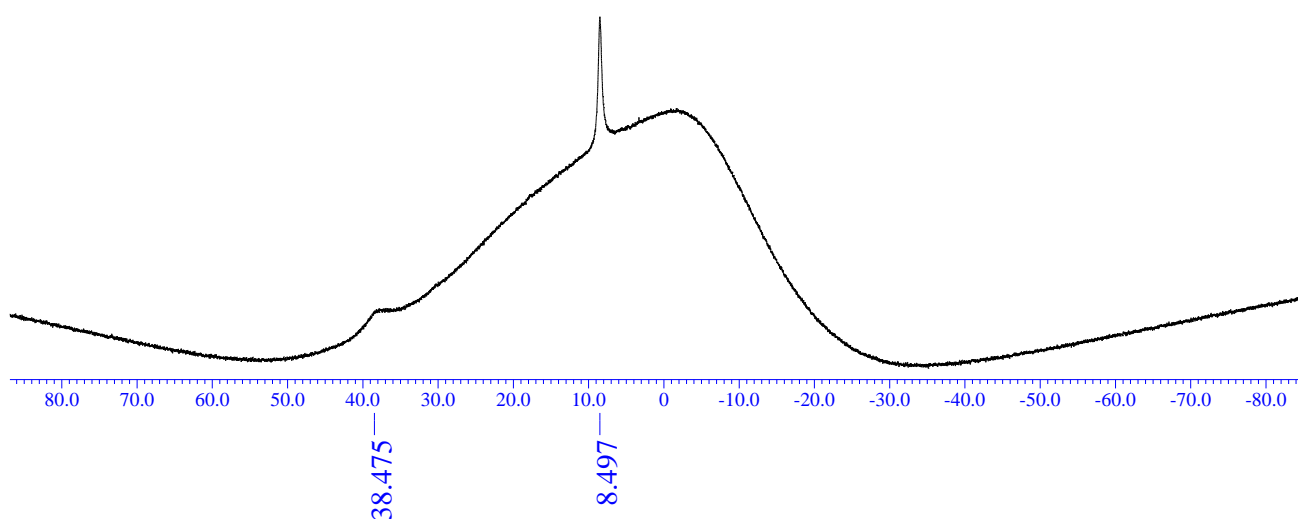
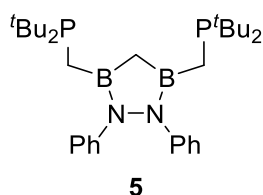


Figure S6. $^{11}\text{B}\{^1\text{H}\}$ NMR spectrum of compound **4** ($\text{THF-}d_8$, 160 MHz).

1,2-diphenyl-3,5-bis(di-*tert*-butylphosphinomethyl)-1,2-diaza-3,5-diborolane (**5**)



To a solution of **4** (2.15 g, 5.34 mmol) in diethyl ether (70 mL), di-*tert*-butylphosphinometyllithium (1.50 g, 9.02 mmol) was added at $-35\text{ }^\circ\text{C}$. The mixture was settled at $-35\text{ }^\circ\text{C}$ for 15 min, then stirred at room temperature for 19 h. The solvent was removed under reduced pressure. The residue was extracted with

hexane. Recrystallization from diethyl ether afforded the desired compound **5** as colourless crystals. The obtained crystals were washed with cold pentane and dried under vacuum (1.04 g, 43% yield).

^1H NMR (500 MHz, C_6D_6) δ : 7.17 (d, 4H, overlapped with benzene), 6.98 (t, $J = 7.3$ Hz, 4H), 6.74 (t, $J = 7.3$ Hz, 2H), 1.55 (s, 2H), 1.29 (d, $J = 4.3$ Hz, 4H), 1.05 (d, $J = 10.7$ Hz, 36H); ^{13}C NMR (126 MHz, C_6D_6) δ : 142.8 (s, 2C), 128.5 (s, 2C), 125.8 (s, 4C), 124.8 (s, 2C), 31.5 (d, $J = 25.8$ Hz, 4C), 29.8 (d, $J = 14.3$ Hz, 12C), 18.5 (br, 1C), 10.3 (br, d, $J = 32.4$ Hz, 2C); $^{11}\text{B}\{^1\text{H}\}$ NMR (160 MHz, C_6D_6) δ : 49.2; $^{31}\text{P}\{^1\text{H}\}$ NMR (202 MHz, C_6D_6) δ : 33.5; Elem. Anal. calcd for $\text{C}_{31}\text{H}_{52}\text{B}_2\text{N}_2\text{P}_2$ C, 69.42; H, 9.77; N, 5.22; found C, 69.19; H, 9.61; N, 5.23; IR (neat) cm^{-1} 2938, 2860, 1598, 1490.

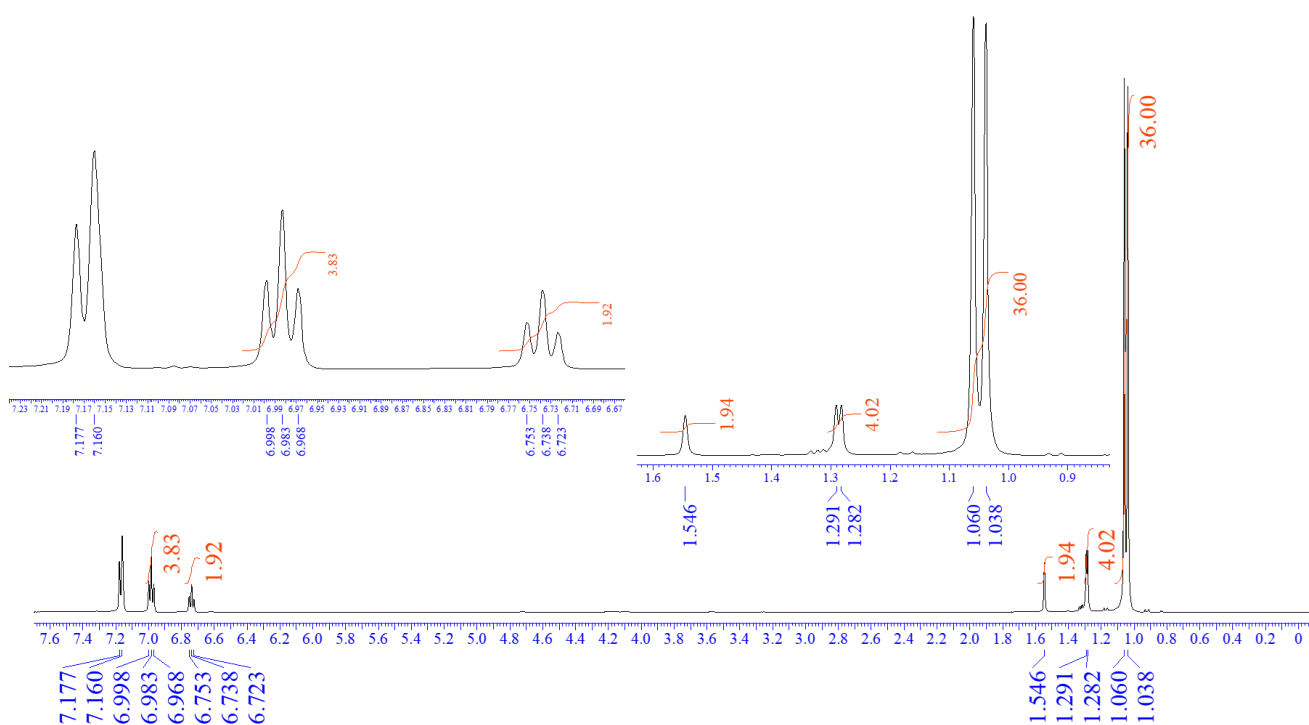


Figure S7. ^1H NMR spectrum of compound **5** (C_6D_6 , 500 MHz).

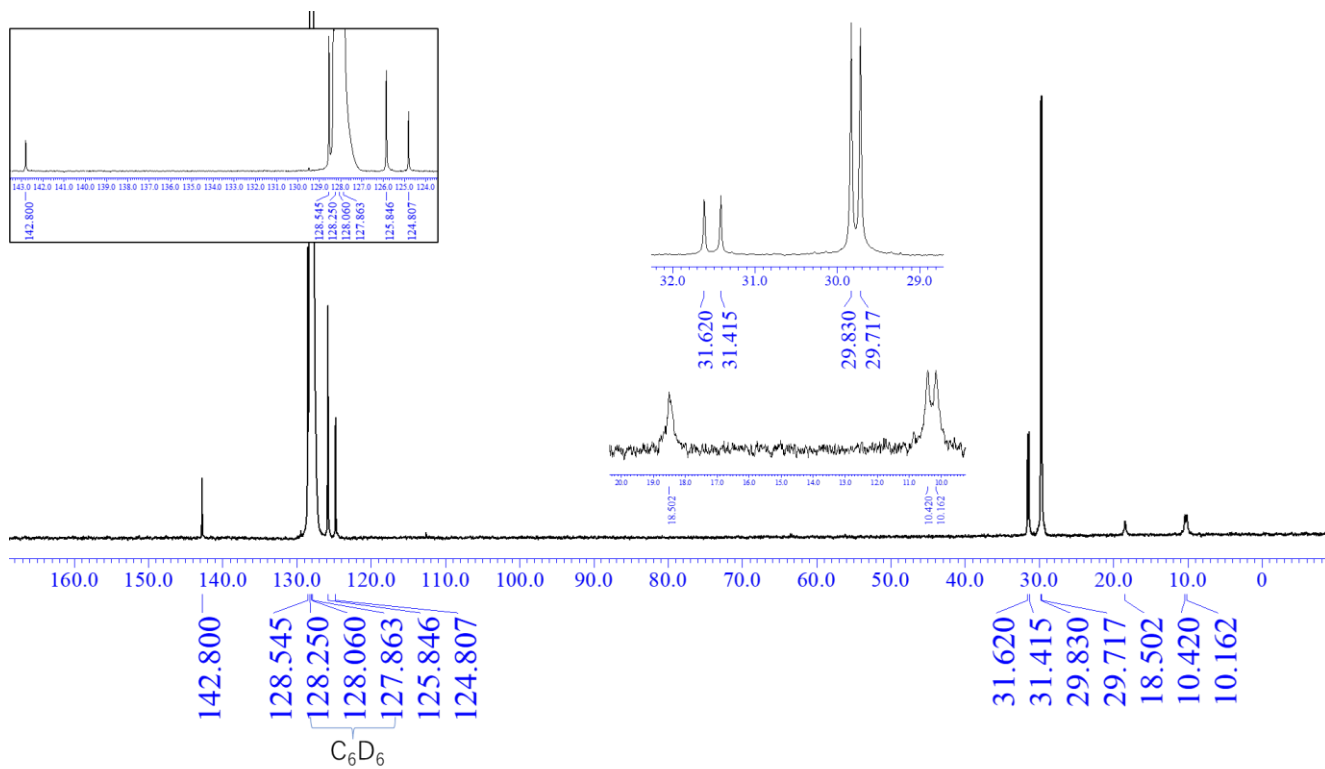


Figure S8. ^{13}C NMR spectrum of compound **5** (C_6D_6 , 126 MHz).

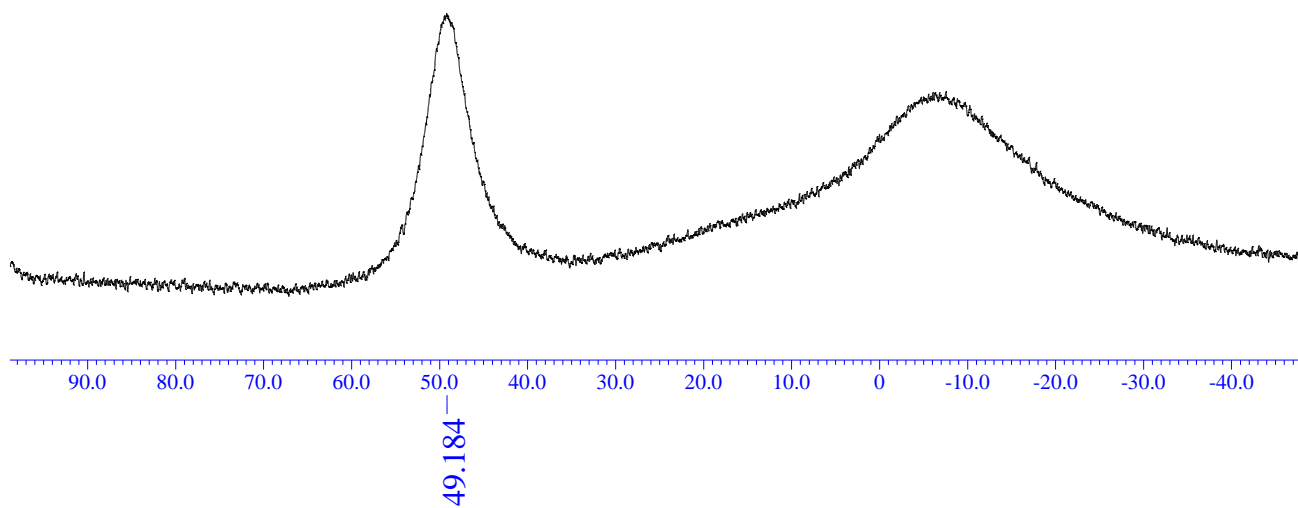


Figure S9. $^{11}\text{B}\{^1\text{H}\}$ NMR spectrum of compound **5** (C_6D_6 , 160 MHz).

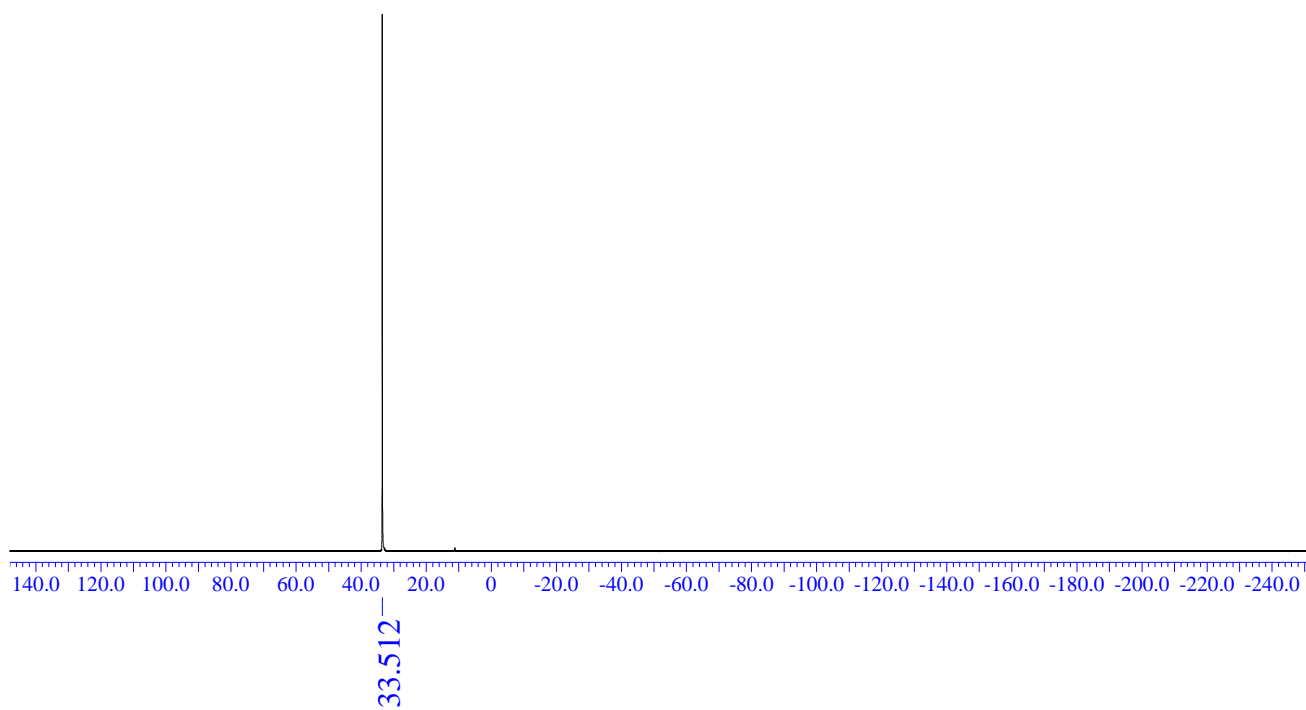
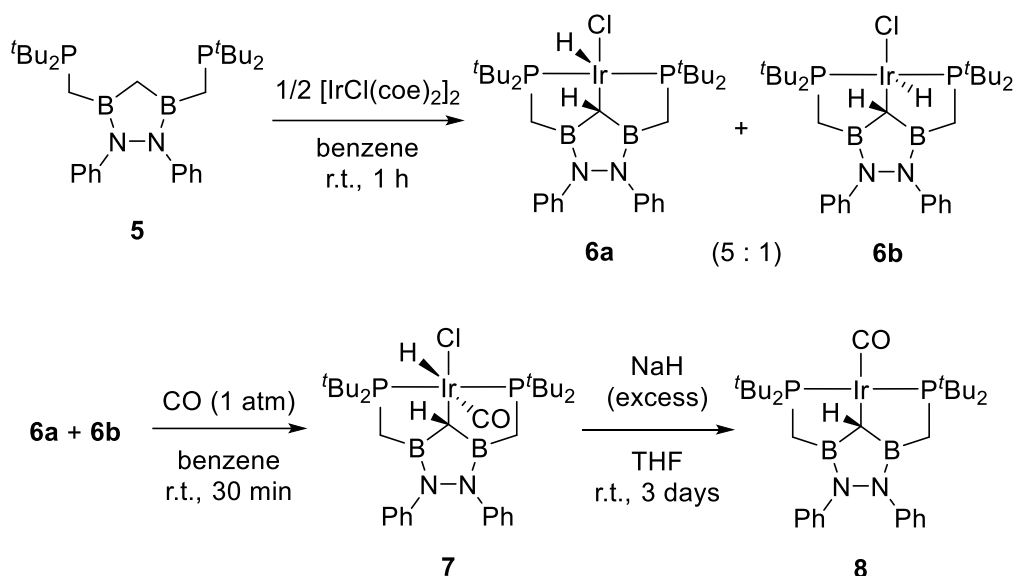
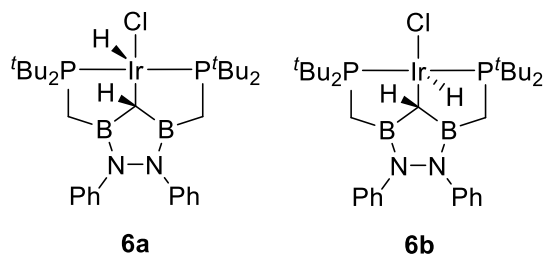


Figure S10. $^{31}\text{P}\{^1\text{H}\}$ NMR spectrum of compound **5** (C_6D_6 , 202 MHz).



Scheme S2. The entire synthetic routes for complexes **6a**, **6b**, **7**, and **8**.

6a and 6b



To a solution of compound **5** (203.0 mg, 0.3784 mmol) in benzene (20 mL), chloridobis(cyclooctene)iridium dimer (169.6 mg, 0.1892 mmol) was added at room temperature. The mixture was stirred at room temperature for 2 h. All the volatiles were removed under reduced pressure to afford the mixture of two isomers of iridium hydride chloride complexes **6a** and **6b** as red solid (279.3 mg, 97% yield in total). Recrystallization from this mixture by slow evaporation of the pentane solution afforded crystals of **6a** and **6b** mixture. Single crystal of **6b** could be obtained after sublimation of the mixture of **6a** and **6b** at 200°C followed by successive recrystallization from benzene/pentane and the structure was determined by single crystal X-ray diffraction analysis. Because **6a** and **6b** were inseparable in chromatographic technique, both are characterized by NMR as the obtained mixture (**6a**:**6b**=5:1, Figures S11–14) and crude mixture containing **6b** as a major component obtained after sublimation (Figures S15–18).

6a: ^1H NMR (500 MHz, C_6D_6) δ : 7.22 (d, $J = 7.4$ Hz, 4H), 7.06 (t, $J = 7.4$ Hz, 4H), 6.77 (t, $J = 7.4$ Hz, 2H), 2.90 (d, $J = 5.8$ Hz, 1H), 1.97 (dvt, $J = 14.8, 5.8$ Hz, 2H), 1.42 (m, 2H), 1.35 (vt, $J = 6.8$ Hz, 18H), 1.28 (vt, $J = 6.8$ Hz, 18H), -47.48 (dt, $J = 5.8, 11.7$ Hz, 1H); ^{13}C NMR (126 MHz, C_6D_6) δ : 144.7 (s, 2C), 128.9 (s, 4C), 122.8 (s, 2C), 121.9 (s, 4C), 38.0 (vt, $J = 8.2$ Hz, 2C), 35.8 (vt, $J = 8.2$ Hz, 2C), 30.5 (s, 6C), 28.6 (s, 6C), 11.4 (br, 1C), 2.7 (br, 2C); $^{11}\text{B}\{^1\text{H}\}$ NMR (160 MHz, C_6D_6) δ : 44.8; $^{31}\text{P}\{^1\text{H}\}$ NMR (202 MHz, C_6D_6) δ : 8.0 (d, $J = 12.4$ Hz).

6b: ^1H NMR (500 MHz, C_6D_6) δ : 7.25 (d, $J = 7.4$ Hz, 4H), 7.08 (t, $J = 7.4$ Hz, 4H), 6.76 (t, $J = 7.4$ Hz, 2H), 3.30 (s, 1H), 1.96 (dvt, $J = 14.8, 5.8$ Hz, 2H), 1.39 (vt, $J = 6.6$ Hz, 18H), 1.17 (vt, $J = 6.6$ Hz, 18H), 1.11 (m, 2H), -44.73 (t, $J = 5.8, 11.7$ Hz, 1H); ^{13}C NMR (126 MHz, C_6D_6) δ : 144.7 (s, 2C), 128.9 (s, 4C), 122.8 (s, 2C), 121.9 (s, 4C), 38.0 (vt, $J = 8.2$ Hz, 2C), 35.8 (vt, $J = 8.2$ Hz, 2C), 30.5 (s, 6C), 28.6 (s, 6C), 11.4 (br, 1C), 2.7 (br, 2C); $^{11}\text{B}\{^1\text{H}\}$ NMR (160 MHz, C_6D_6) δ : 44.8; $^{31}\text{P}\{^1\text{H}\}$ NMR (202 MHz, C_6D_6) δ : 8.0 (d, $J = 12.4$ Hz).

= 11.3 Hz, 1H); ^{13}C NMR (126 MHz, C_6D_6) δ : 145.3 (s, 2C), 129.0 (s, 4C), 122.7 (s, 2C), 121.4 (s, 4C), 37.9 (vt, J = 7.3 Hz, 2C), 35.6 (vt, J = 9.5 Hz, 2C), 29.9 (s, 6C), 29.6 (s, 6C), 17.0(br, 1C), 4.8 (br, 2C); $^{11}\text{B}\{^1\text{H}\}$ NMR (160 MHz, C_6D_6) δ : 48.8; $^{31}\text{P}\{^1\text{H}\}$ NMR (202 MHz, C_6D_6) δ : 15.4 (d, J = 10.0 Hz).

Mixture of **6a** and **6b**: Elem. Anal. calcd for $\text{C}_{31}\text{H}_{52}\text{B}_2\text{N}_2\text{P}_2\text{ClIr}$ C, 48.74; H, 6.86; N, 3.67; found C, 48.43; H, 6.98; N, 3.35; IR (neat) cm^{-1} 2896, 1937, 1597, 1488.

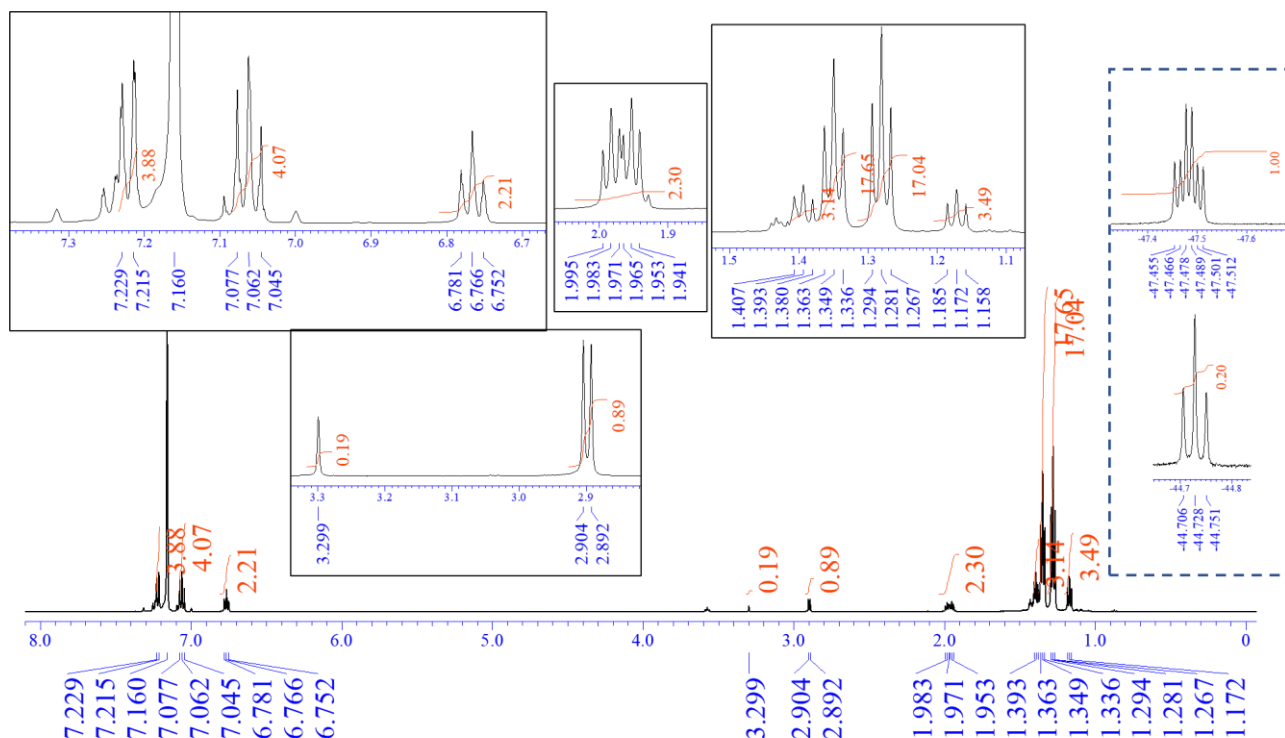


Figure S11. ^1H NMR spectrum of compounds **6a** and **6b** (6a:6b=5:1, C_6D_6 , 500 MHz). Hydride region is separately shown in the dashed box.

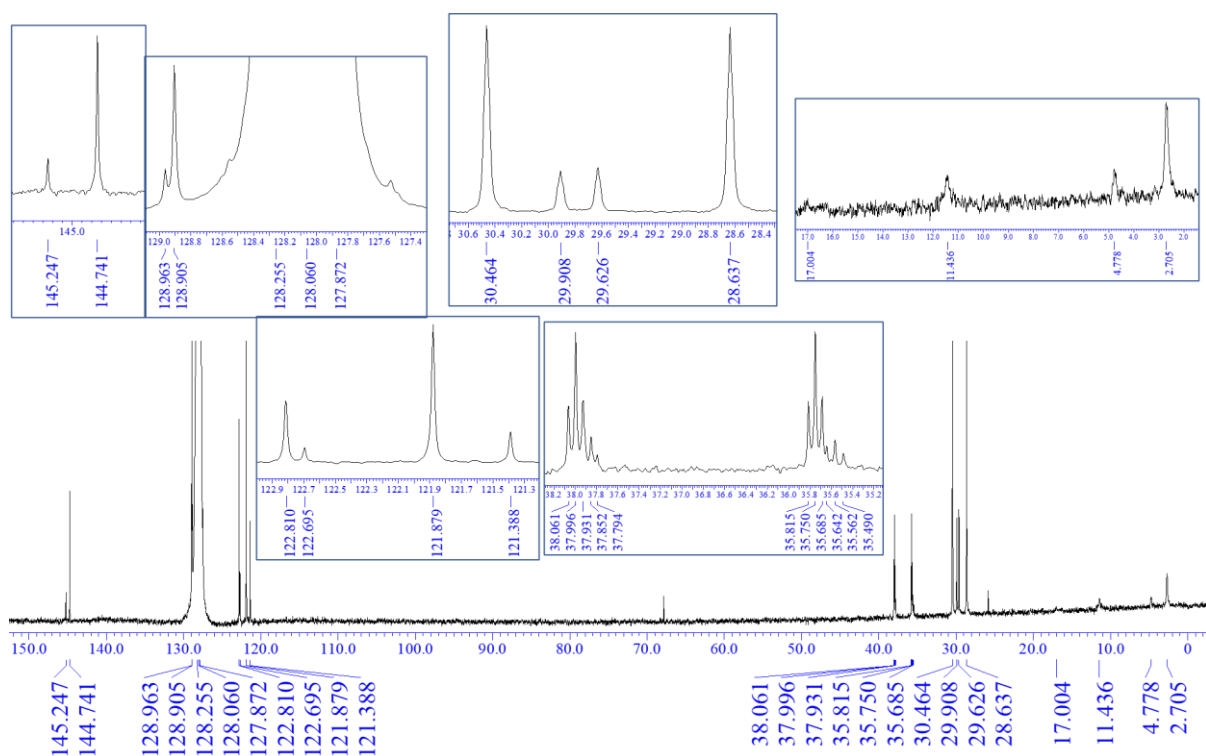


Figure S12. ^{13}C NMR spectrum of compounds **6a** and **6b** (6a:6b=5:1, C_6D_6 , 126 MHz).

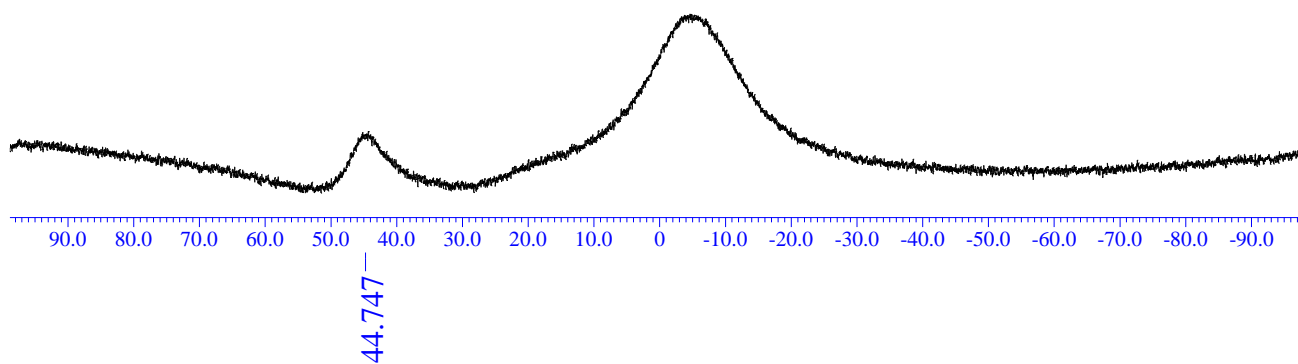


Figure S13. $^{11}\text{B}\{^1\text{H}\}$ NMR spectrum of compounds **6a** and **6b** (**6a:6b**=5:1, C_6D_6 , 160 MHz).

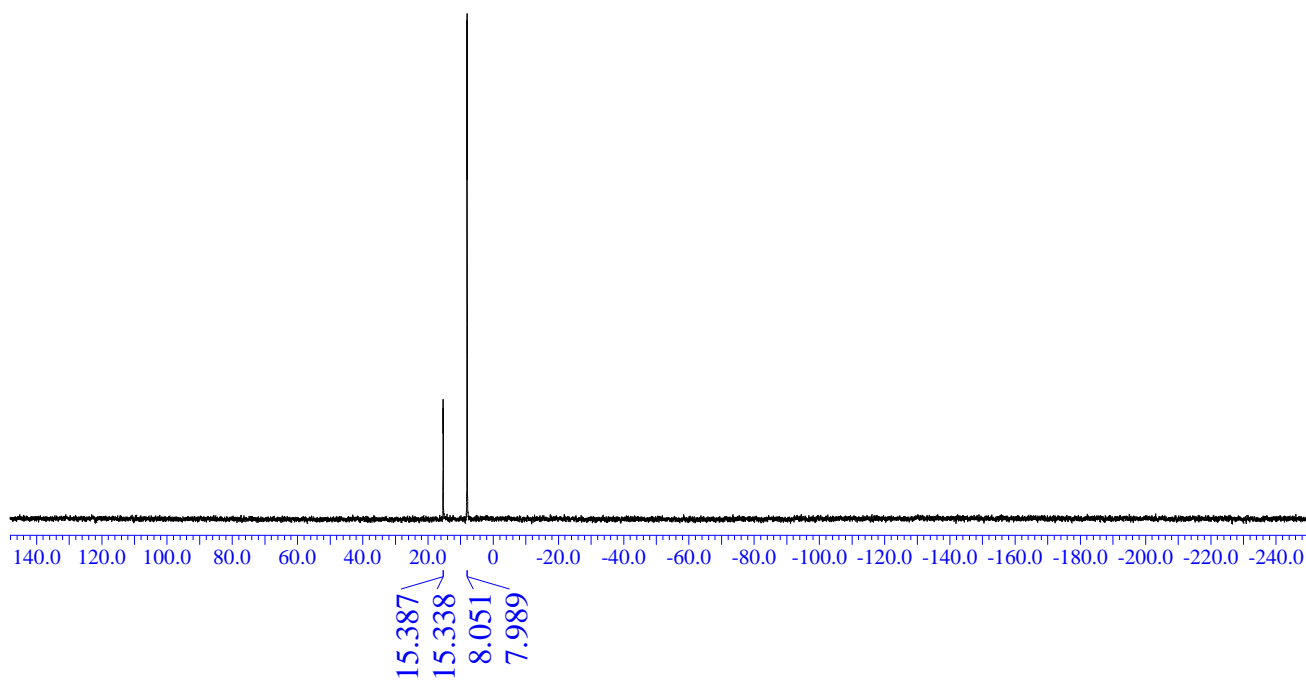


Figure S14. $^{31}\text{P}\{^1\text{H}\}$ NMR spectrum of compounds **6a** and **6b** (**6a:6b**=5:1, C_6D_6 , 202 MHz).

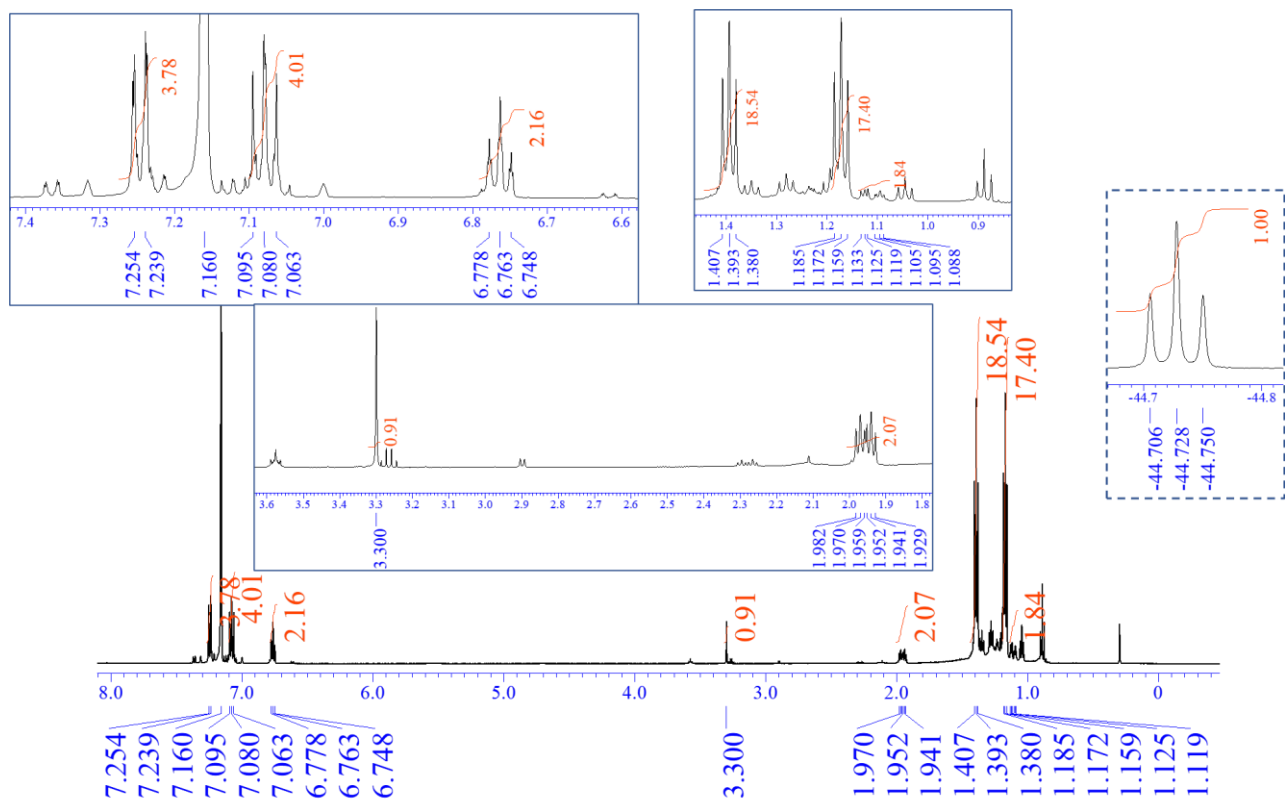


Figure S15. ^1H NMR spectrum of the crude product after sublimation containing **6b** as the main component (C_6D_6 , 500 MHz). Hydride region is separately shown in the dashed box.

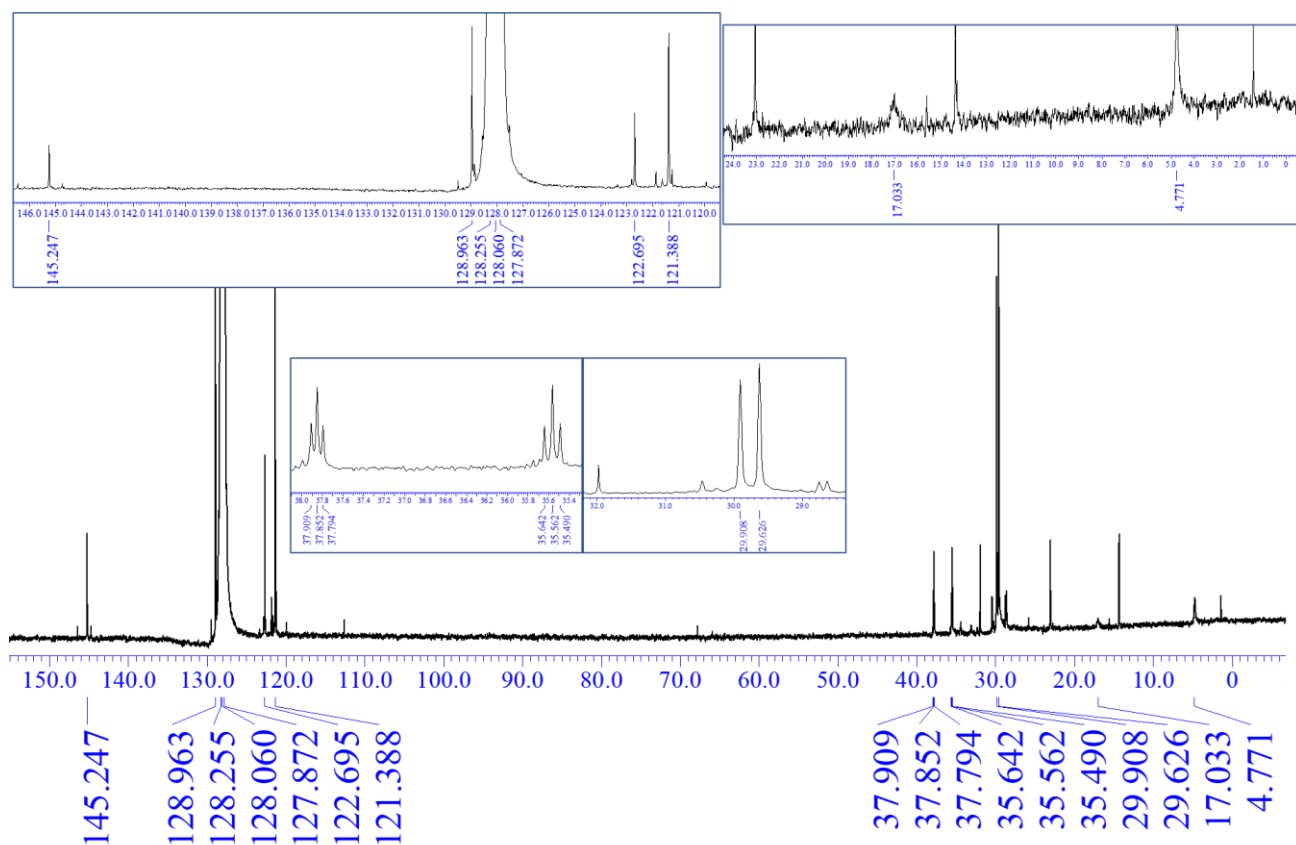


Figure S16. ^{13}C NMR spectrum of the crude product after sublimation containing **6b** as the main component (C_6D_6 , 126 MHz).

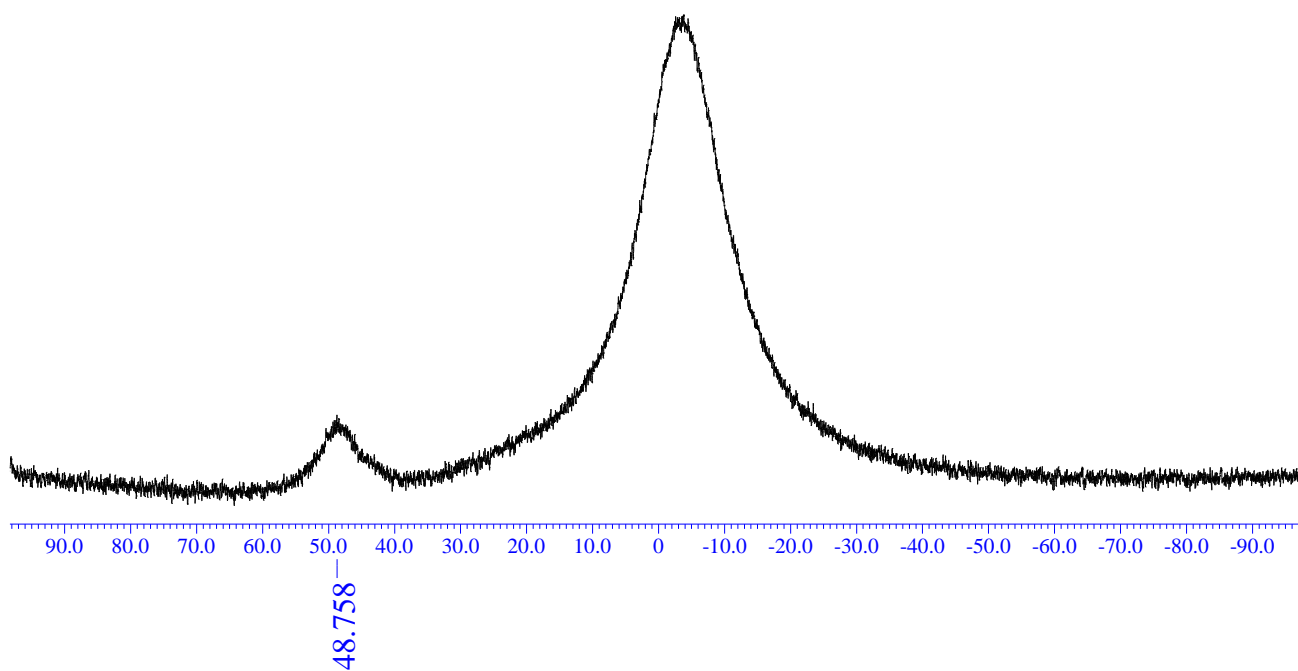


Figure S17. $^{11}\text{B}\{^1\text{H}\}$ NMR spectrum of the crude product after sublimation containing **6b** as the main component (C_6D_6 , 160 MHz).

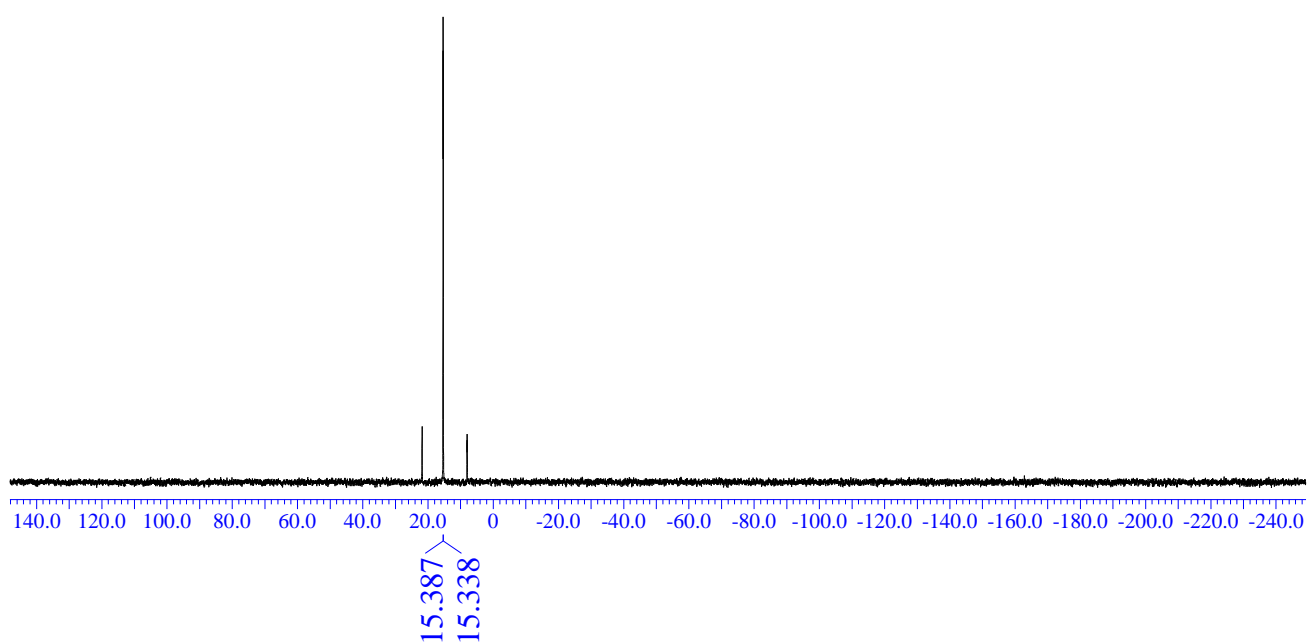
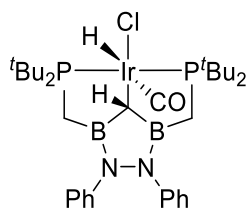


Figure S18. $^{31}\text{P}\{^1\text{H}\}$ NMR spectrum of the crude product after sublimation containing **6b** as the main component (C_6D_6 , 202 MHz).



7

To a Schlenk tube which contained a solution of the mixture of compounds **6a** and **6b** (100.3 mg, 0.1313 mmol) in benzene (10 mL), ambient pressure of carbon monoxide was introduced. The solution was stirred at room temperature for 1 hour. After removal of the volatiles, complex **7** was obtained as pale-yellow solid (103.2 mg, 99% yield). This solid could be further purified by recrystallization from the toluene/pentane solution.

NMR spectra were recorded at 15 °C because **7** was gradually decomposed in the C₆D₆ solution at ambient temperature.

¹H NMR (500 MHz, C₆D₆) δ: 7.21 (d, *J* = 7.4 Hz, 4H), 7.05 (t, *J* = 7.4 Hz, 4H), 6.78 (t, *J* = 7.4 Hz, 2H), 2.12 (dvt, *J* = 15.9, 5.2 Hz, 2H), 1.94 (d, *J* = 1.9 Hz, 1H), 1.42 (vt, *J* = 6.8 Hz, 18H), 1.36 (vt, *J* = 7.2 Hz, 18H), 1.10 (dvt, *J* = 2.4, 16.2 Hz, 2H), -6.74 (td, *J* = 15.8, 2.1 Hz, 1H); ¹³C NMR (126 MHz, C₆D₆) δ: 182.6 (s, 1C), 142.9 (s, 2C), 128.8 (s, 4C), 123.5 (s, 2C), 123.4 (s, 4C), 38.2 (vt, *J* = 8.1 Hz, 2C), 37.3 (vt, *J* = 11.0 Hz, 2C), 31.3 (s, 6C), 28.7 (s, 6C), 11.0 (br, 1C), 6.0 (br, 2C); ¹¹B{¹H} NMR (160 MHz, C₆D₆) δ: 46.5; ³¹P{¹H} NMR (202 MHz, C₆D₆) δ: 10.0 (s); Elem. Anal. calcd for C₃₂H₅₂B₂N₂OP₂ClIr C, 48.53; H, 6.62; N, 3.54; found C, 48.47; H, 6.70; N, 3.33; IR (neat) cm⁻¹ 2899, 2157, 1986, 1597.

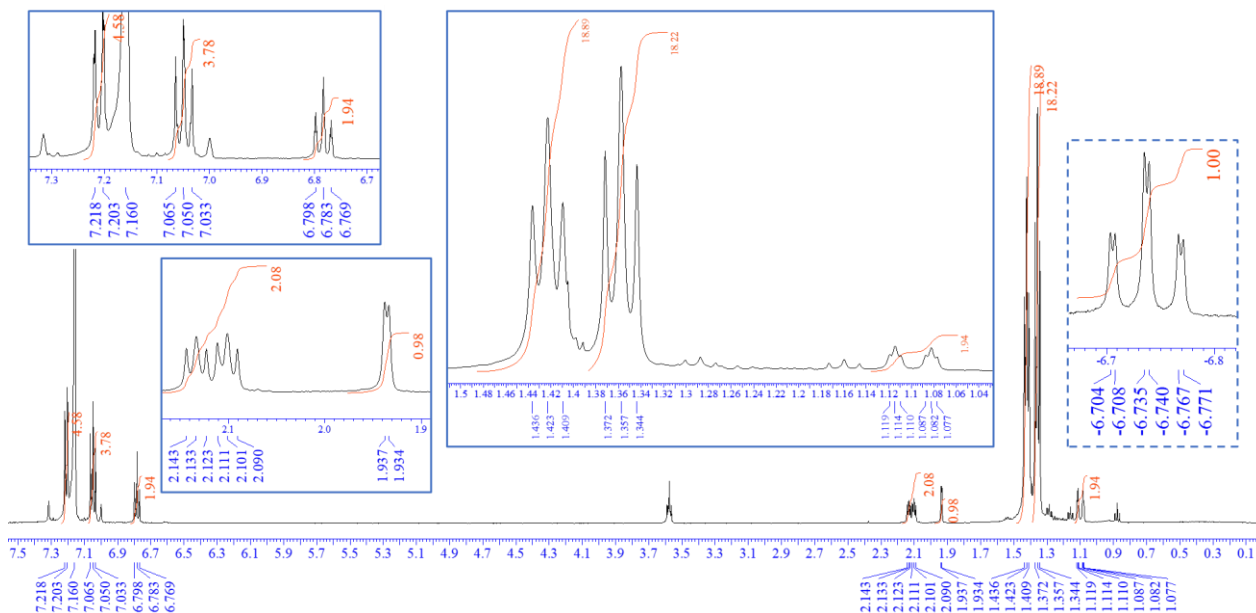


Figure S19. ¹H NMR spectrum of **7** (C₆D₆, 500 MHz). Hydride region is separately shown in the dashed box.

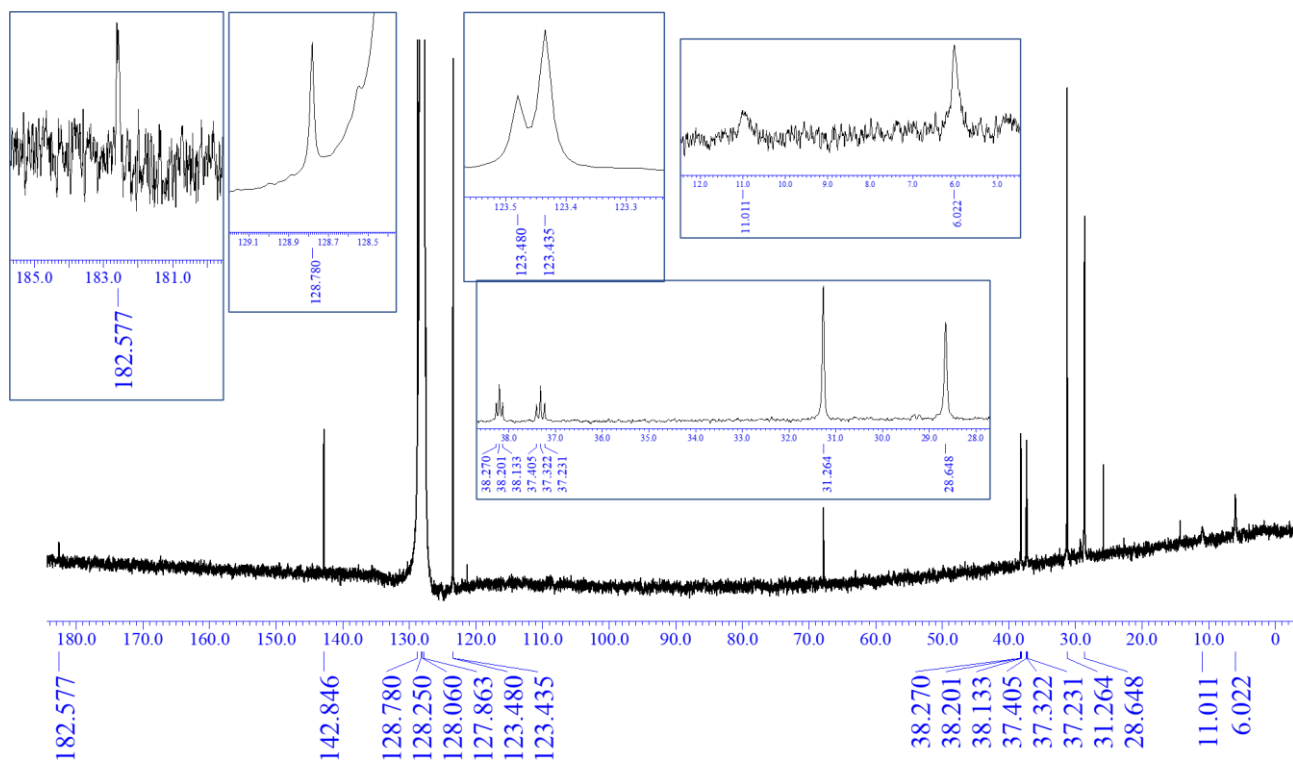


Figure S20. ^{13}C NMR spectrum of **7** (C_6D_6 , 126 MHz).

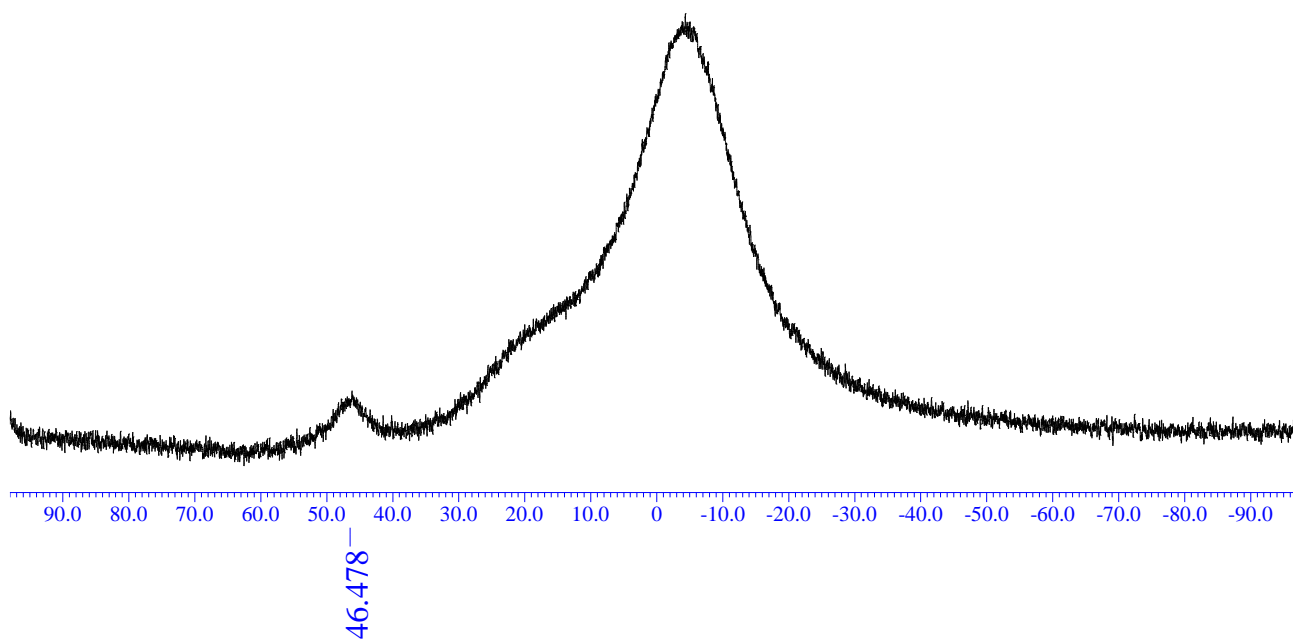


Figure S21. $^{11}\text{B}\{^1\text{H}\}$ NMR spectrum of **7** (C_6D_6 , 160 MHz).

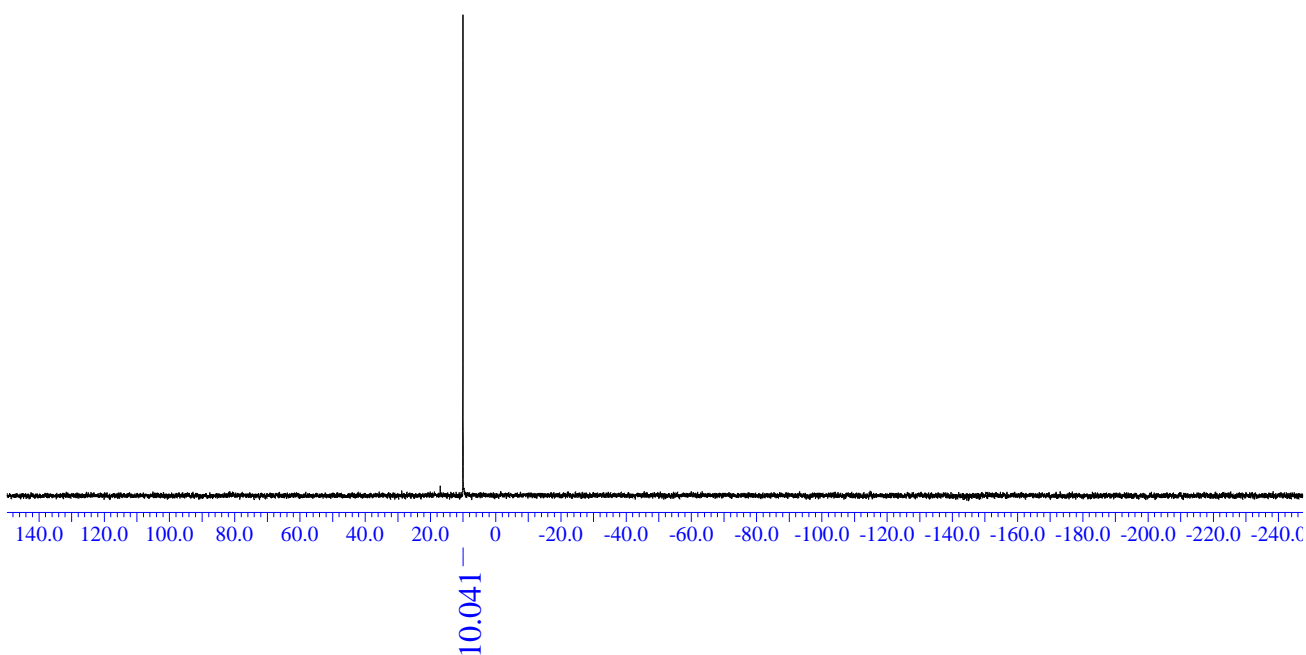
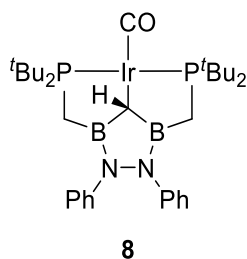


Figure S22. $^{31}\text{P}\{^1\text{H}\}$ NMR spectrum of **7** (C_6D_6 , 202 MHz).

8



To a solution of complex **7** (49.8 mg, 62.9 μmol) in THF (7 mL), sodium hydride (28.5 mg, 1.19 mmol) was added. The mixture was stirred vigorously at room temperature for 3 days. After removal of insoluble species by filtration, the solvent was removed under reduced pressure. Complex **8** was obtained as yellow solid (45.9 mg, 97% yield). The solid can be further purified by recrystallization from the toluene/pentane solution.

Generation of complex **8** was also observed by heating complex **7** at 40dC in C_6D_6 solution. A portion of complex **7** was dissolved in C_6D_6 in a sealed J-Young NMR tube, then heated to 30°C. Conversion of **7** was confirmed by ^1H and ^{31}P NMR analyses. The peak area of methine proton was employed and silicon grease was used for internal standard for quantitative analysis. After 4 days of heating, 91% conversion of **7** and generation of complex **8** was confirmed (38% yield). Decomposition products other than complex **8** could not be identified (see Figure S27 and S28).

^1H NMR (500 MHz, C_6D_6) δ : 7.29 (d, $J = 7.6$ Hz, 4H), 7.10 (t, $J = 7.6$ Hz, 4H), 6.77 (t, $J = 7.6$ Hz, 2H), 2.36 (s, 1H), 2.10 (dvt, $J = 15.3, 4.6$ Hz, 2H), 1.35 (dvt, $J = 15.3, 4.6$ Hz, 2H), 1.29 (vt, $J = 6.4$ Hz, 18H), 1.17 (vt, $J = 6.4$ Hz, 18H); ^{13}C NMR (126 MHz, C_6D_6) δ : 184.1 (s, 1C), 145.6 (s, 2C), 128.9 (s, 4C), 122.1 (s, 2C), 121.4 (s, 4C), 52.6 (br, 1C), 35.9 (vt, $J = 10.4$ Hz, 2C), 35.6 (vt, $J = 10.4$ Hz, 2C), 29.4 (s, 6C), 29.3 (s, 6C), 3.0 (br, 2C); $^{11}\text{B}\{^1\text{H}\}$ NMR (160 MHz, C_6D_6) δ : 45.9; $^{31}\text{P}\{^1\text{H}\}$ NMR (202 MHz, C_6D_6) δ : 17.1; Elem. Anal. calcd for $\text{C}_{32}\text{H}_{51}\text{B}_2\text{N}_2\text{OP}_2\text{Ir}$ C, 50.87; H, 6.80; N, 3.71; found C, 50.84; H, 7.04; N, 3.45; IR (neat) cm^{-1} 2898, 1967, 1904, 1597.

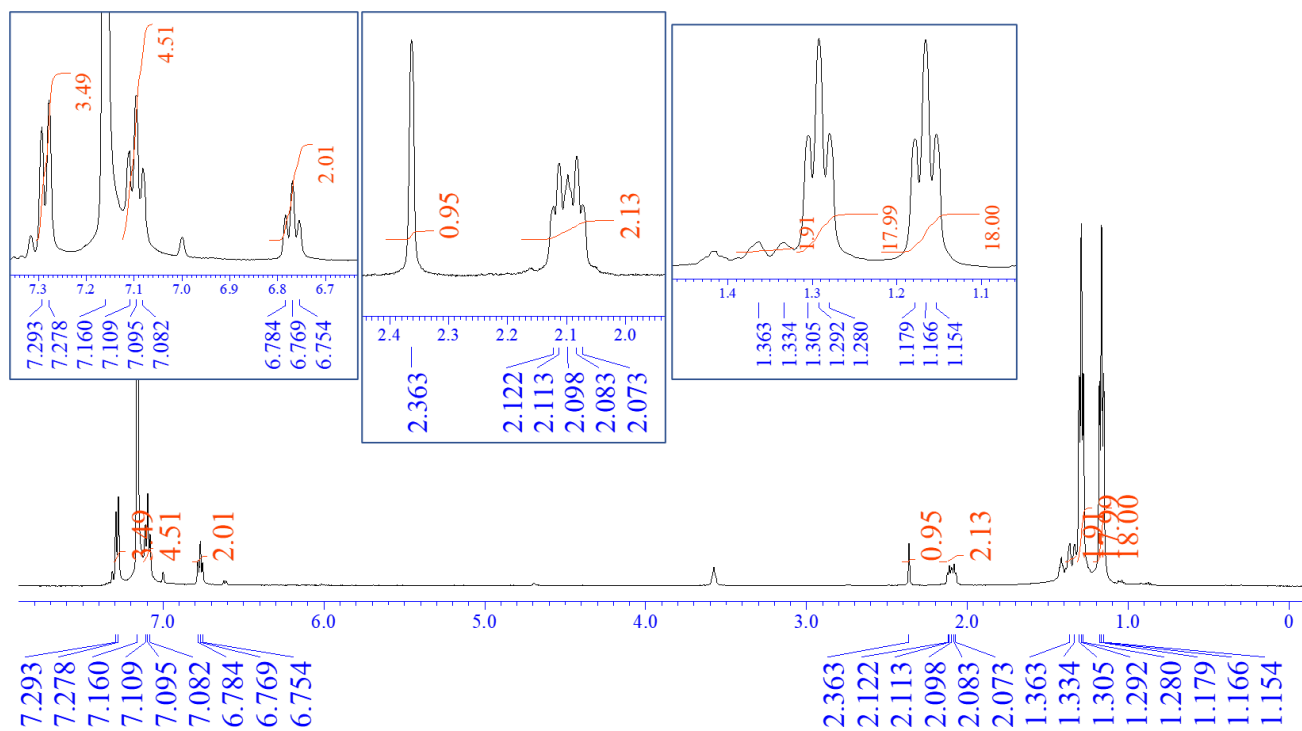


Figure S23. ^1H NMR spectrum of **8** (C_6D_6 , 500 MHz).

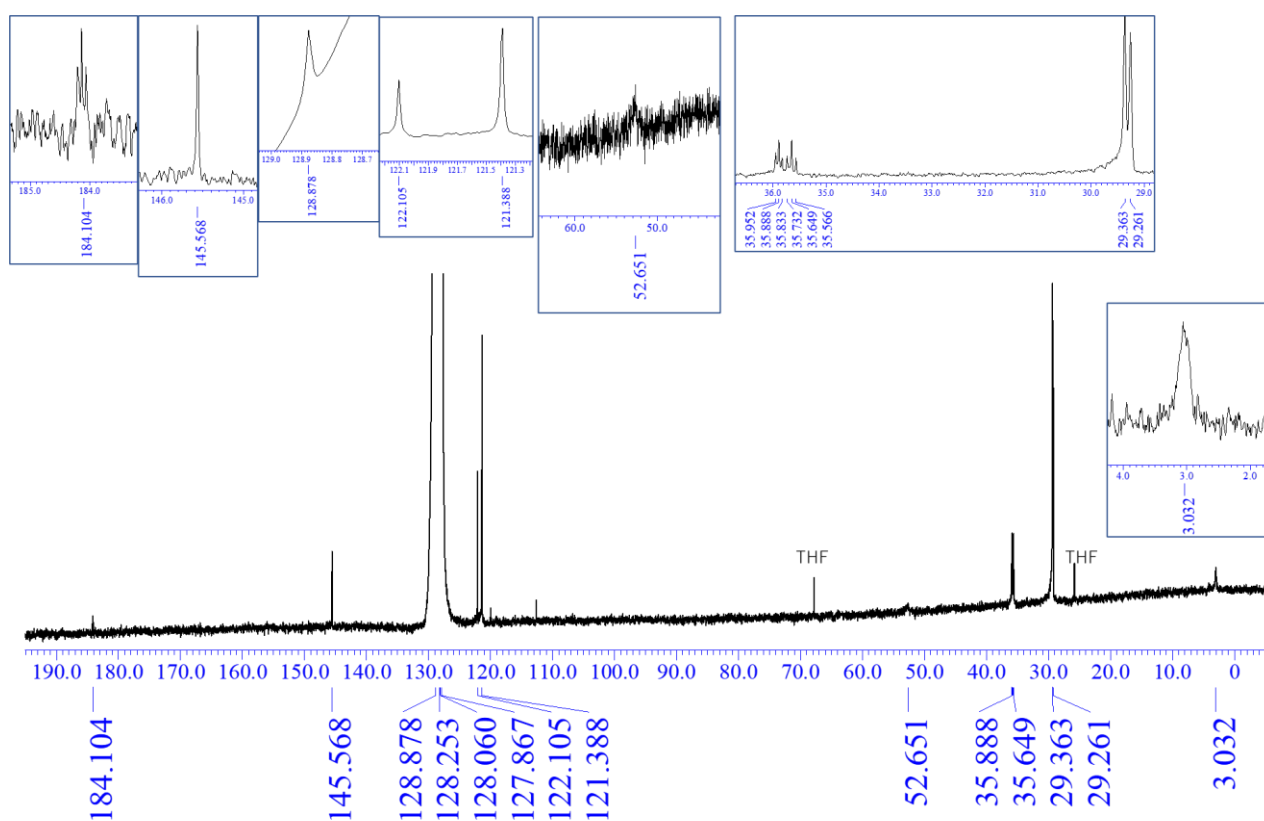


Figure S24. ^{13}C NMR spectrum of **8** (C_6D_6 , 126 MHz).

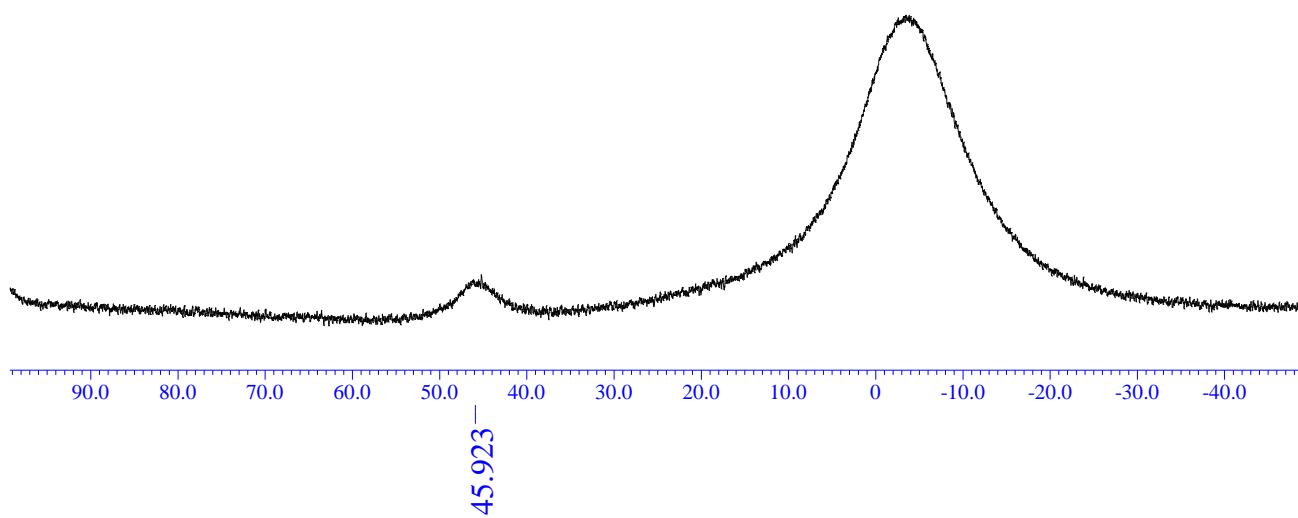


Figure S25. $^{11}\text{B}\{^1\text{H}\}$ NMR spectrum of **8** (C_6D_6 , 160 MHz).

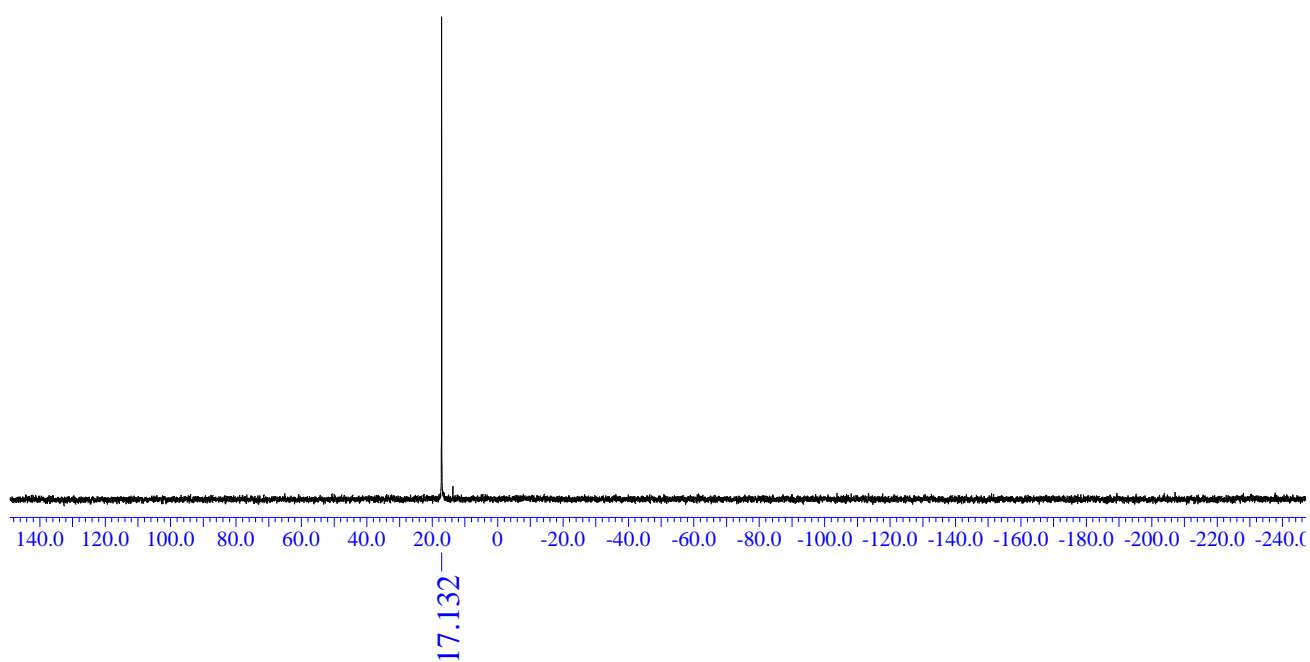


Figure S26. $^{31}\text{P}\{^1\text{H}\}$ NMR spectrum of **8** (C_6D_6 , 202 MHz).

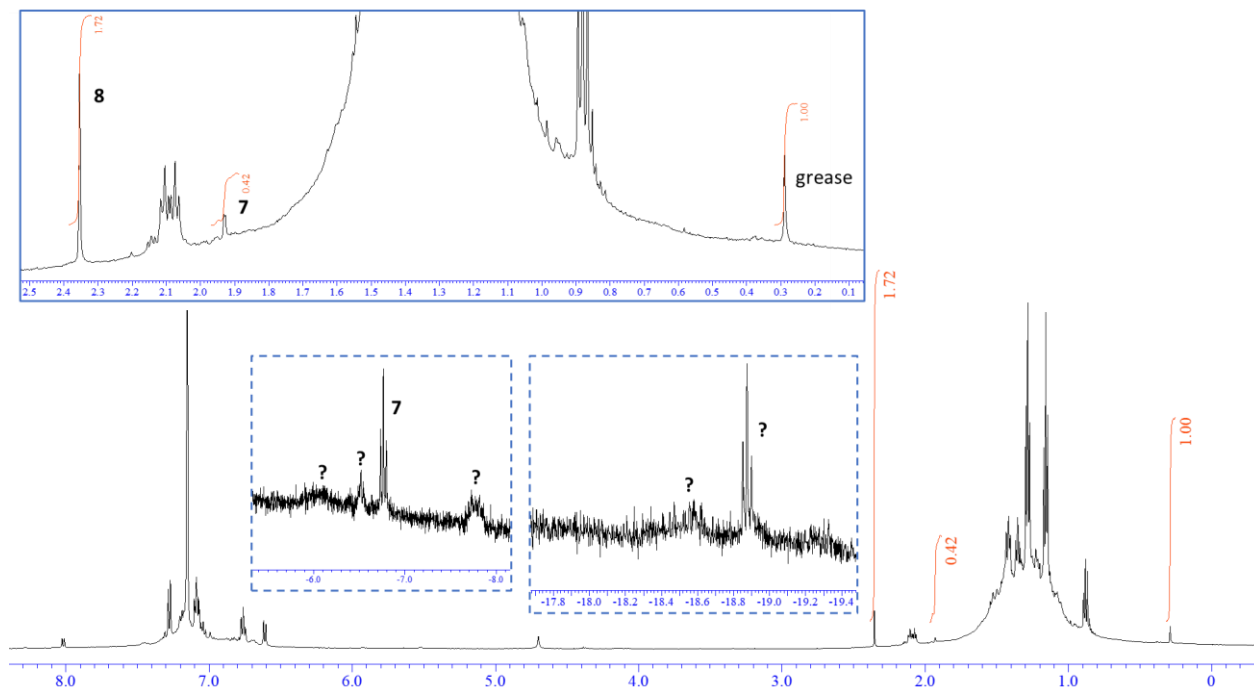


Figure S27. ^1H NMR spectrum after heating complex 7 (C_6D_6 , 500 MHz). Hydride region is separately shown in the dashed boxes.

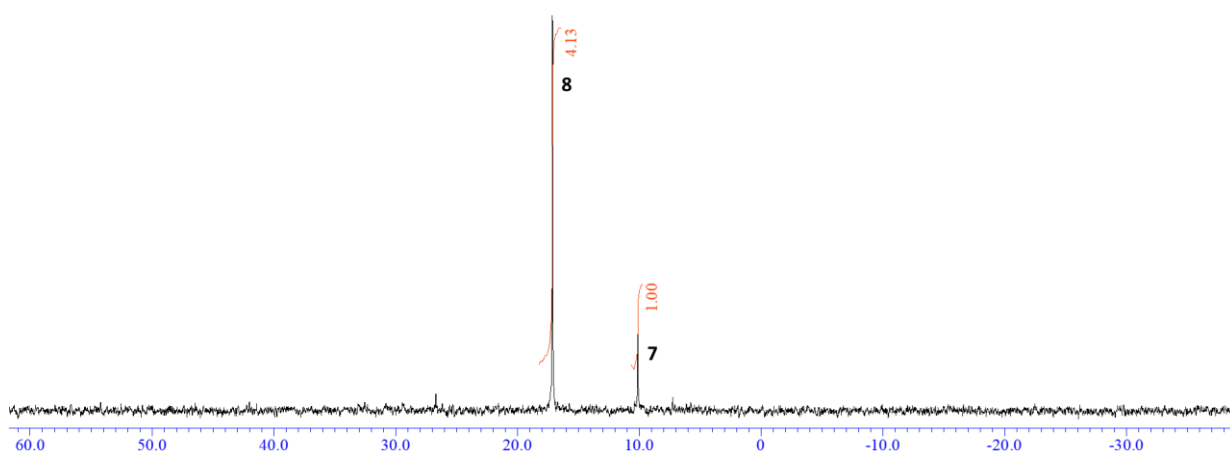
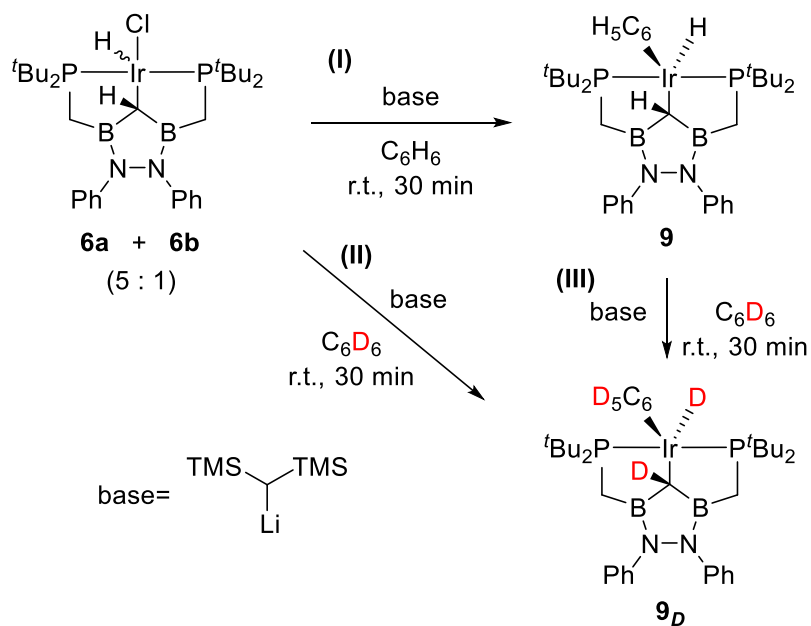
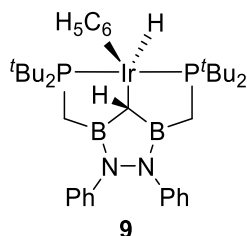


Figure S28. $^{31}\text{P}\{^1\text{H}\}$ NMR spectrum after heating complex 7 (C_6D_6 , 202 MHz).



Scheme S3. The entire synthetic routes for complexes **9** and **9_D**.

9



[Reaction (I) in NMR scale]

The reaction was conducted in a valved NMR tube under argon atmosphere. To a solution of the mixture of **6a** and **6b** (10.0 mg, 13.1 μmol) in benzene (0.5 mL), bis(trimethylsilyl)methyl lithium (4.2 mg, 25.2 μmol) was added. The mixture was settled at room temperature for 30 min. By NMR analyses, generation of compound **9** was confirmed.

[Reaction (I) in large scale]

To a solution of the mixture of **6a** and **6b** (30.6 mg, 40.1 μmol) in benzene (5 mL), bis(trimethylsilyl)methyl lithium (13.4 mg, 80.1 μmol) was added. The mixture was stirred at room temperature for 30 min. The solution was concentrated to *ca.* 0.5 mL. Complex **9** was recrystallized by the addition of pentane slowly with vapor-diffusion method to afford orange crystals. The obtained crystals were washed with pentane and dried under reduced pressure to afford pure complex **9** (6.0 mg, 19 % yield).

Because complex **9** gradually decomposed in solvents other than C₆H₆, NMR spectra could successfully be recorded only in C₆H₆ (with solvent lock and shimming with ¹H signal of C₆H₆).

¹H NMR (400 MHz, C₆H₆) Signals of the aromatic protons were overlapped with the signal of benzene. δ : 2.14 (m, 2H), 1.21 (m, 2H), 1.14 (dd, $J = 10.6, 3.2$ Hz, 1H), 1.07 (m, 18H), 0.98 (m, 18H), -38.19 (dt, $J = 10.6, 9.5$ Hz, 1H); ¹³C NMR (126 MHz, C₆H₆) Signals of the aromatic carbons cannot be assigned because of the noise from the solvent (C₆H₆). δ : 65.9 (br, 1C), 36.2 (s, 4C), 29.8 (s, 6C), 29.4 (s, 6C), 4.5 (br, 2C); ¹¹B{¹H} NMR (160 MHz, C₆H₆) δ : 46.9; ³¹P{¹H} NMR (202 MHz, C₆H₆) δ : 4.7; Elem. Anal. calcd for C₃₇H₅₇B₂N₂P₂Ir C, 55.16; H, 7.13; N, 3.48; found C, 55.04; H, 7.18; N, 3.48; IR (neat) cm⁻¹ 2922, 1597, 1565, 1488.

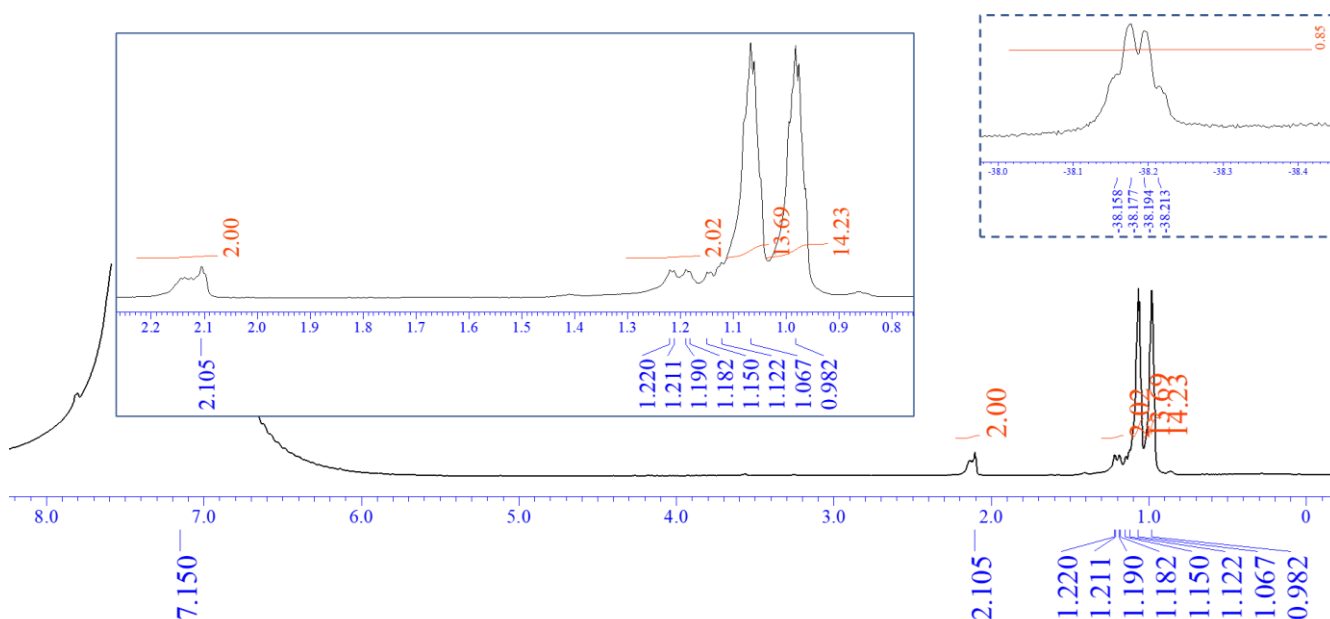


Figure S29. ¹H NMR spectrum of **9** (C₆H₆, 400 MHz). Hydride region is separately shown in the dashed box.

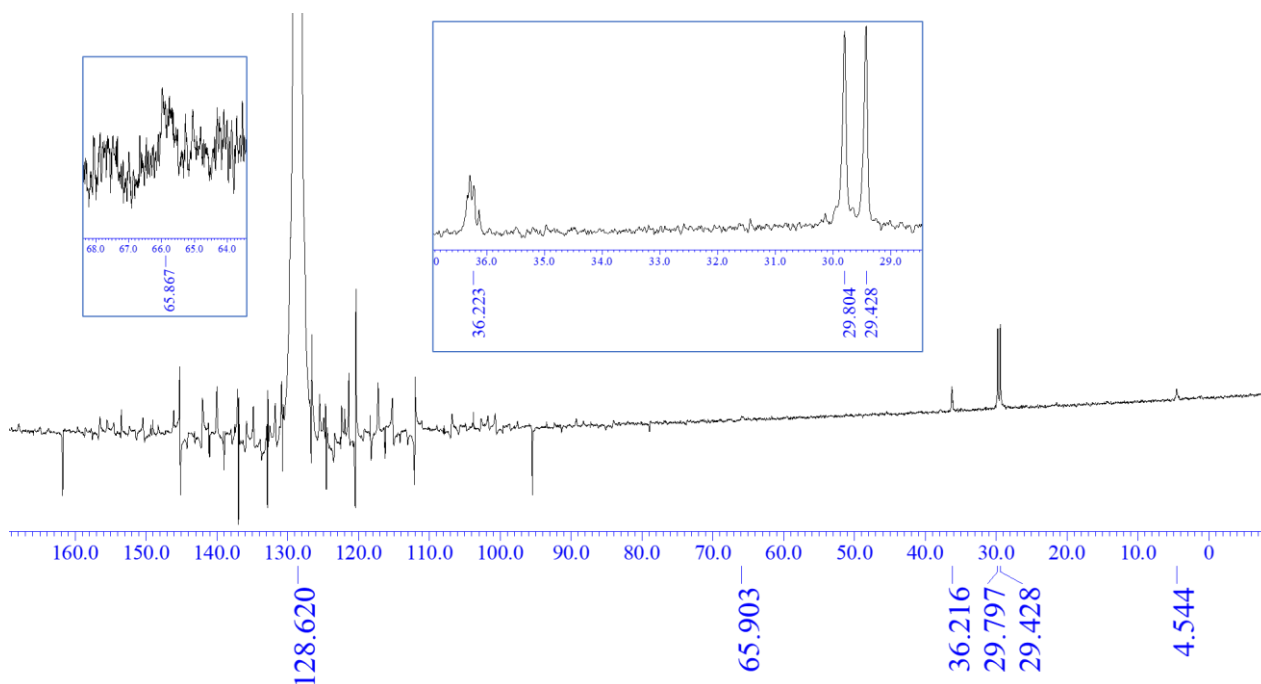


Figure S30. ¹³C NMR spectrum of **9** (C₆H₆, 126MHz).

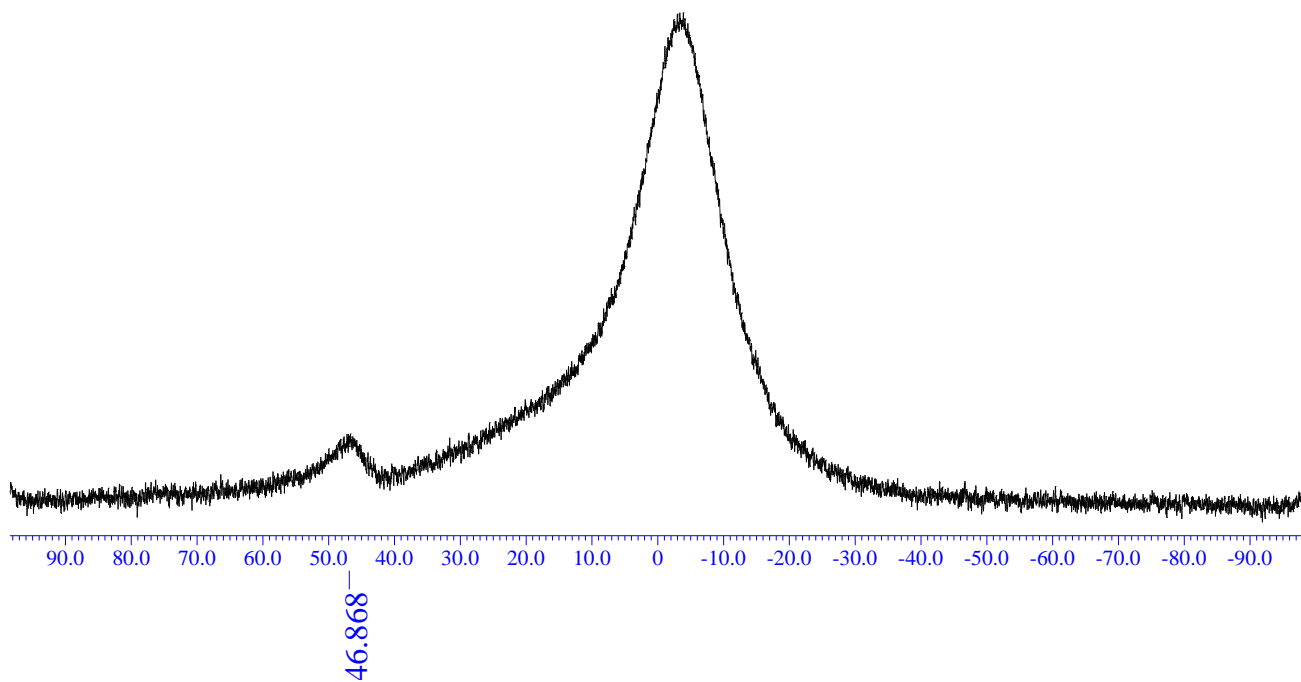


Figure S31. $^{11}\text{B}\{^1\text{H}\}$ NMR spectrum of **9** (C_6H_6 , 160 MHz).

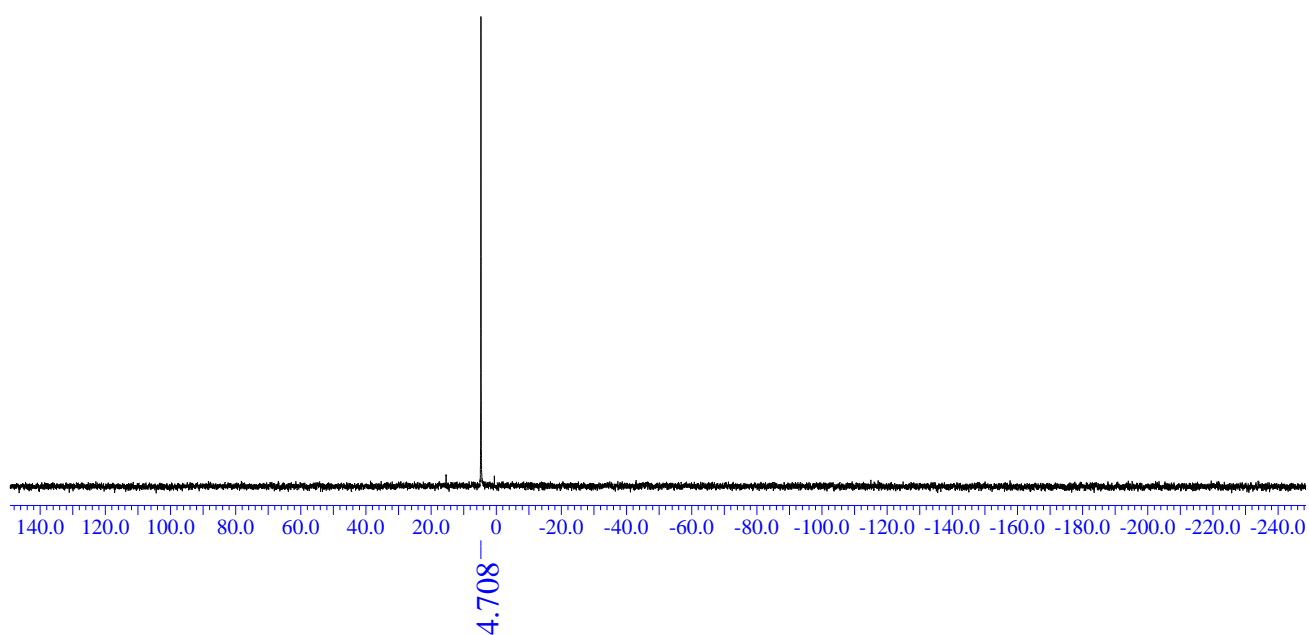
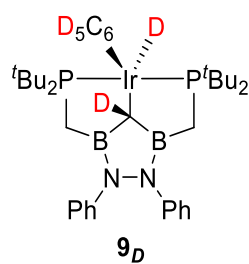


Figure S32. $^{31}\text{P}\{^1\text{H}\}$ NMR spectrum of **9** (C_6H_6 , 202 MHz).

9_D



[Reaction (II)]

The reaction was conducted in an NMR tube. To a solution of the mixture of **6a** and **6b** (5.0 mg, 6.54 μmol) in benzene- d_6 (0.5 mL), bis(trimethylsilyl)methyl lithium (2.2 mg, 13.1 μmol) was added. The mixture was settled at room temperature for 1.5 h. Generation of compound **9_D** was confirmed by ^1H , ^2H and ^{31}P NMR.

[Reaction (III)]

A small portion of crystals of complex **9** was dissolved in benzene- d_6 (0.5 mL) at room temperature. After 30 min, complete conversion of complex **9** to complex **9_D** was confirmed by ^{31}P and ^1H NMR analyses.

^1H NMR (500 MHz, C_6D_6) δ : 7.33 (d, $J = 7.4$ Hz, 4H), 7.13 (t, $J = 7.4$ Hz, 4H), 6.79 (t, $J = 7.4$ Hz, 2H), 2.13 (dvt, $J = 14.8, 4.6$ Hz, 2H), 1.21 (dvt, $J = 14.8, 4.2$ Hz, 2H), 1.08 (vt, $J = 6.4$ Hz, 18H), 0.98 (vt, $J = 6.4$ Hz, 18H); ^{13}C NMR (126 MHz, C_6D_6) δ : 146.0 (s, 2C), 128.9 (s, 4C), 121.9 (s, 2C), 121.3 (s, 4C), 66.6 (br, the signal is quite hard to see because of the coupling with two boron, one deuterium and two phosphorous nuclei), 36.2 (s, 4C), 29.8 (s, 6C), 29.3 (s, 6C), 4.5 (br, 2C); $^{11}\text{B}\{^1\text{H}\}$ NMR (160 MHz, C_6D_6) δ : 47.9; $^{31}\text{P}\{^1\text{H}\}$ NMR (202 MHz, C_6D_6) δ : 4.9; ^2H NMR (61 MHz, C_6D_6) δ : 1.30, -37.5; IR (neat) cm^{-1} 2895, 1592, 1552, 1468.

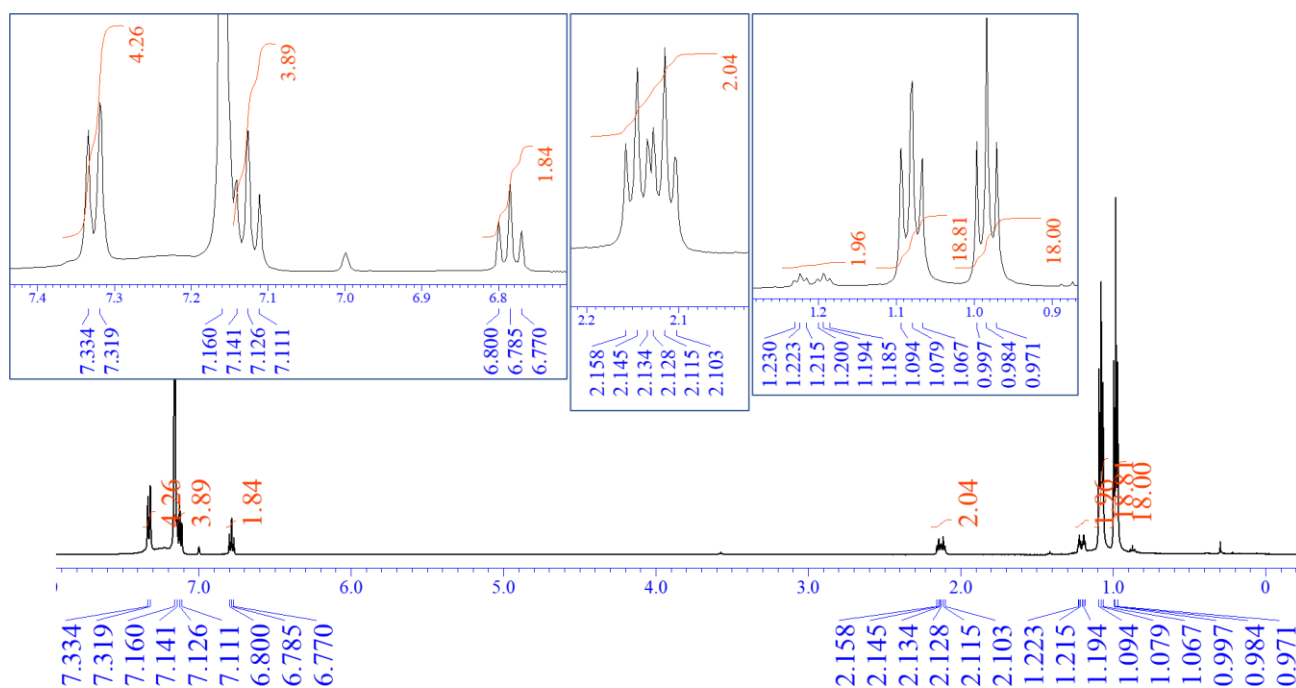


Figure S33. ^1H NMR spectrum of **9_D** (C_6D_6 , 500 MHz).

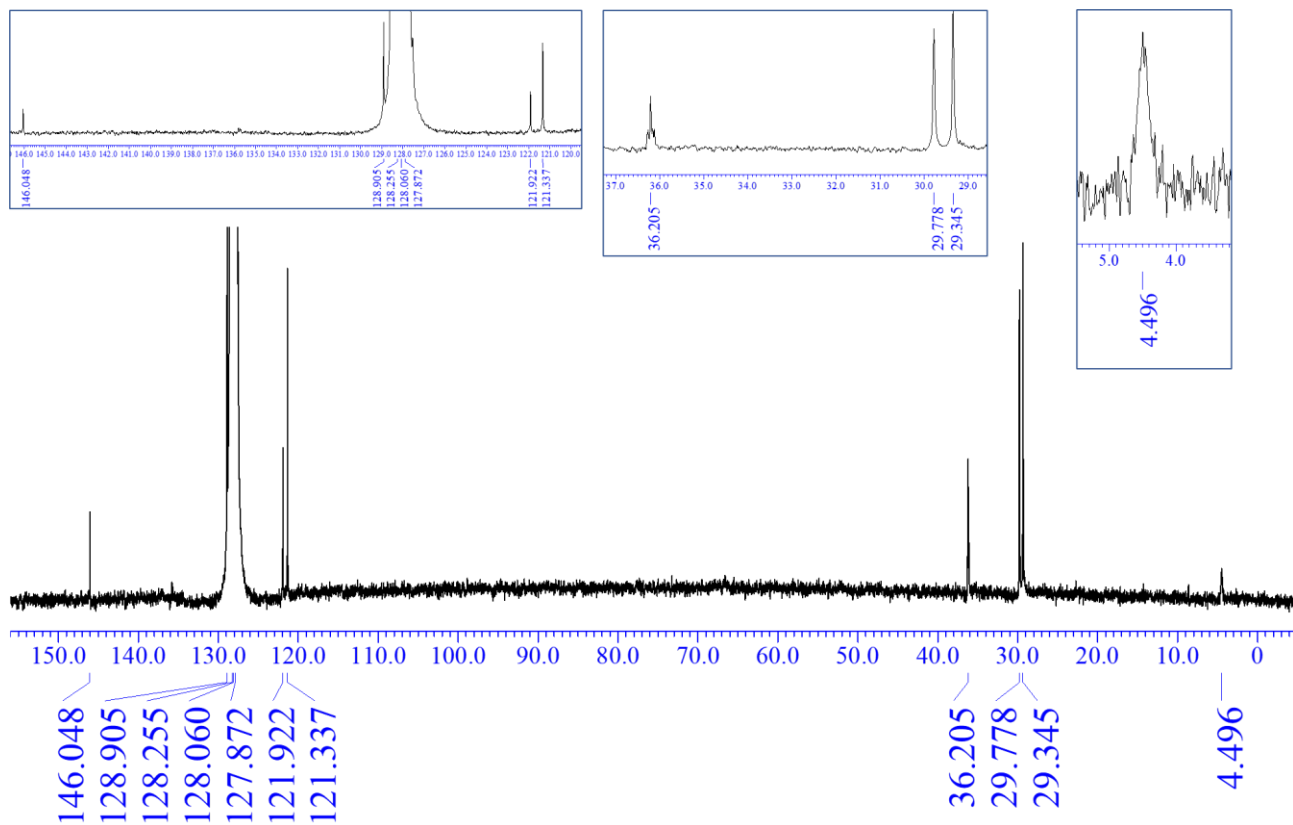


Figure S34. ^{13}C NMR spectrum of 9_D (C_6D_6 , 126 MHz).

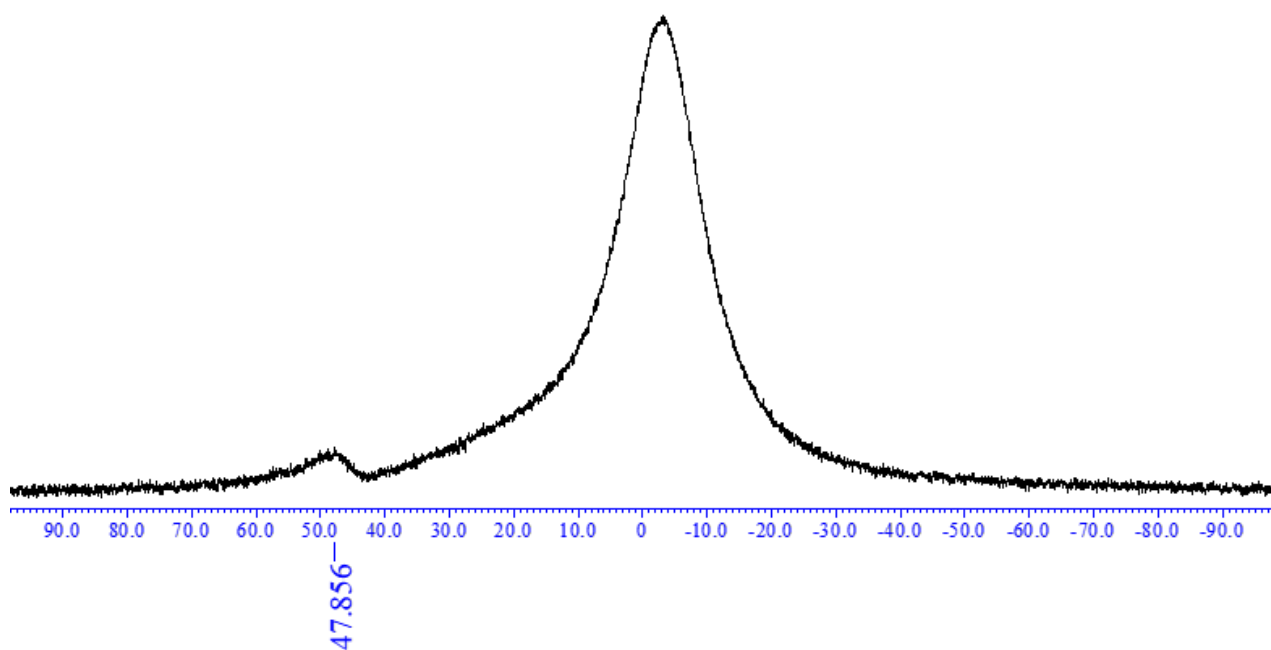


Figure S35. $^{11}\text{B}\{^1\text{H}\}$ NMR spectrum of 9_D (C_6D_6 , 160 MHz).

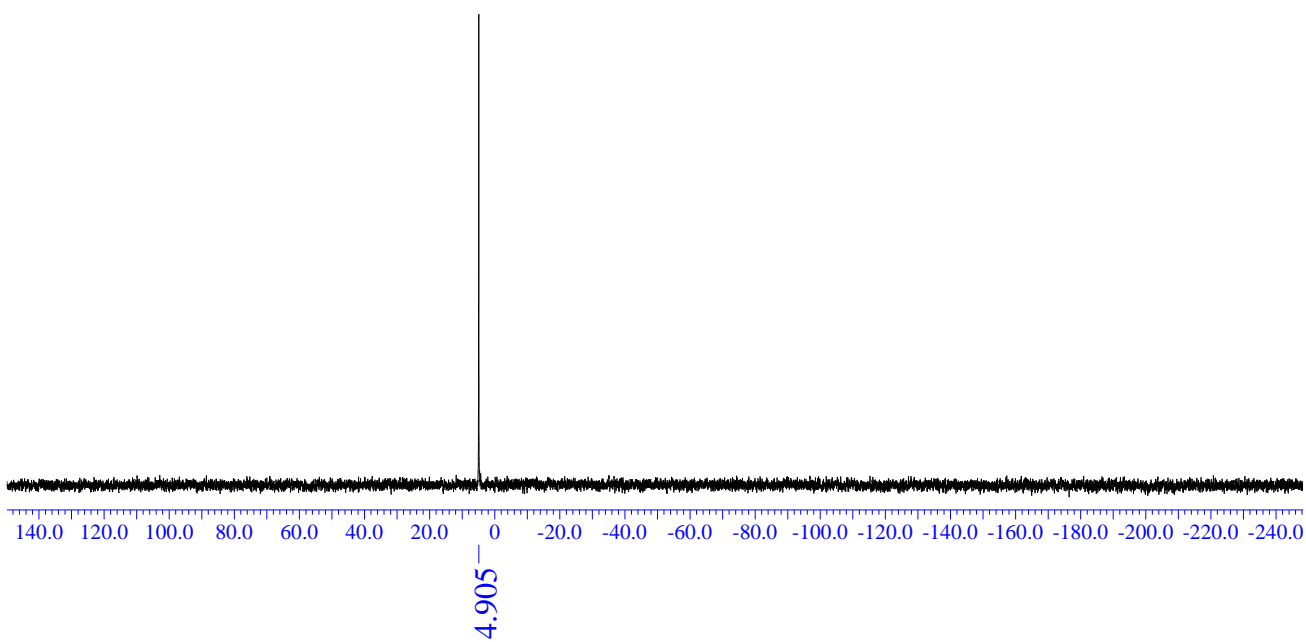


Figure S36. $^{31}\text{P}\{^1\text{H}\}$ NMR spectrum of 9_D (C_6D_6 , 202 MHz).

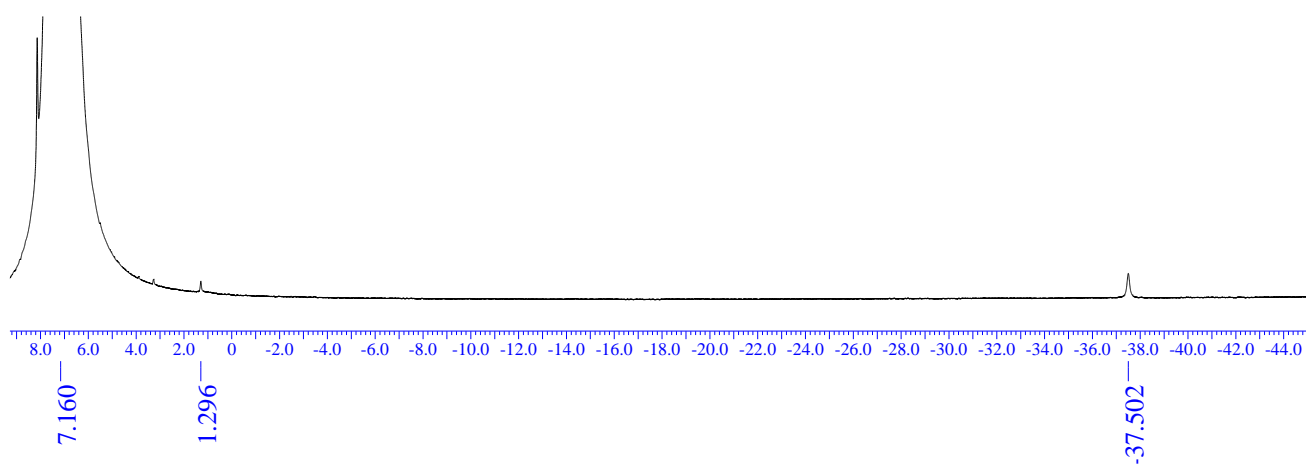
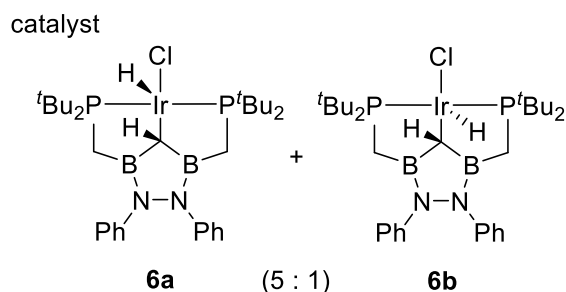
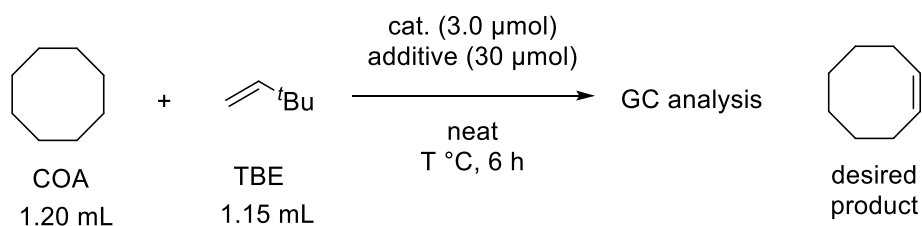


Figure S37. ^2H NMR spectrum of 9_D (C_6D_6 , 61 MHz).

I-III. Dehydrogenation of Cyclooctane

To a 10-mL autoclave, cyclooctane (1.25 mL) and 3,3-dimethylbut-1-ene (*tert*-butylethylene, 1.20 mL), then, 5:1 mixture of complexes **6a** and **6b** (2.3 mg, 3.0 μ mol), and additive (30 μ mol) were added. The autoclave was filled with argon and heated to a certain temperature. After 6 hours, the reaction mixture was analyzed by GC with an internal standard (dodecane). TON was calculated by dividing the obtained amount of cyclooctene with the amount of catalyst used.

Table S1. Dehydrogenation of cyclooctane with the synthesized complexes.



entry	additive	temp. ($^\circ\text{C}$)	TON
1	NaO ^t Bu	200	1.9
2	NaO ^t Bu	140	0.48
3	None	140	0.45

Results and Discussions: Initially the mixture of **6a** and **6b** was examined with an assistant base NaO^tBu (entry 1). TON was low (1.9) and decomposed black iridium powder was precipitated. Under lower temperature (entry 2) and without base (entry 3), TON was still quite low, although decomposed precipitate was not observed. The synthesized PCP-iridium complexes seemed to have only limited activity for transfer dehydrogenation of cycloalkane.

II. IR Spectra of the Novel Compounds

Compound 3

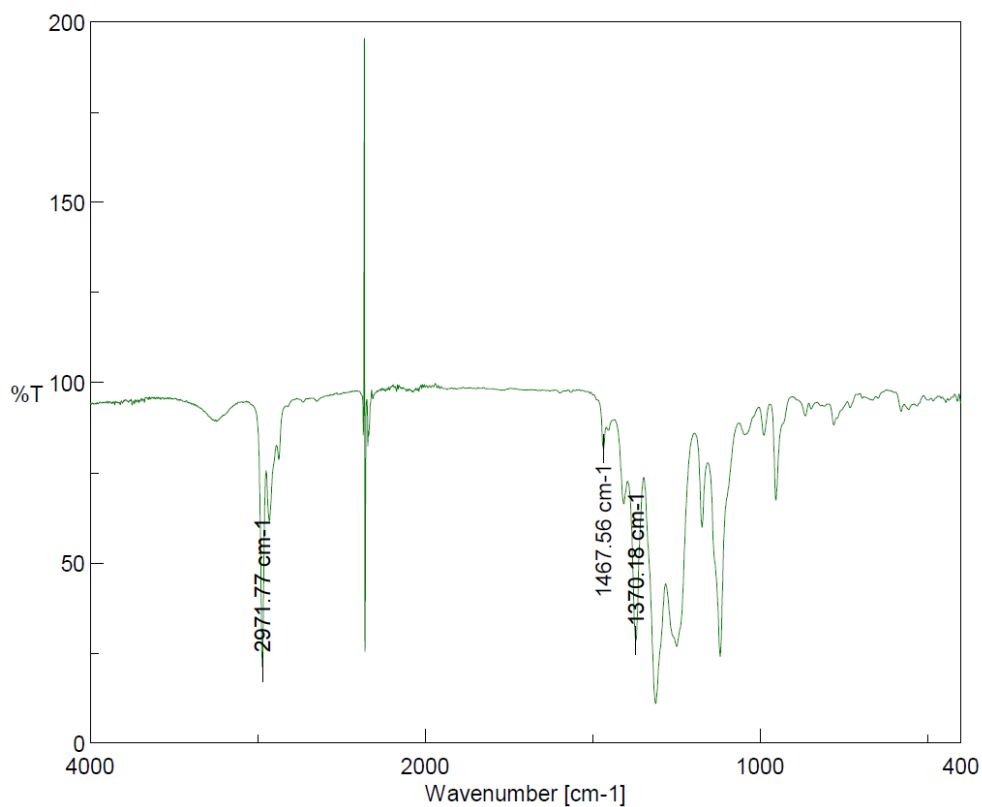


Figure S38. IR spectrum (ATR) for compound 3.

Compound 4

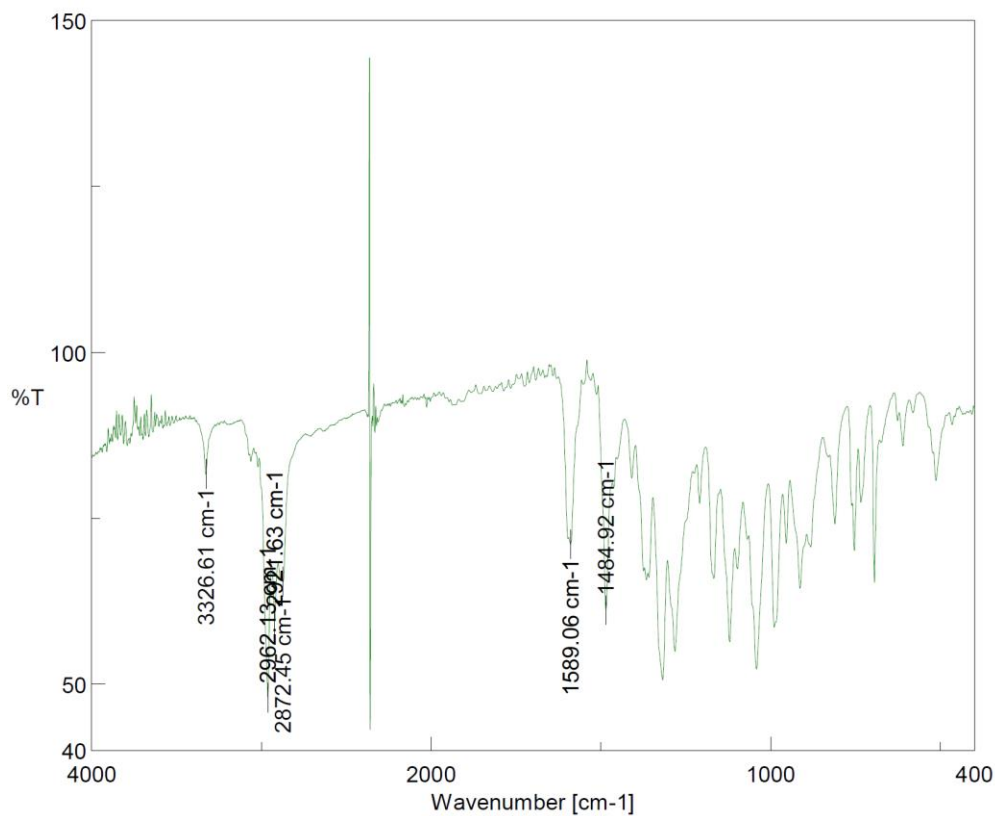


Figure S39. IR spectrum (ATR) for compound 4.

Compound 5

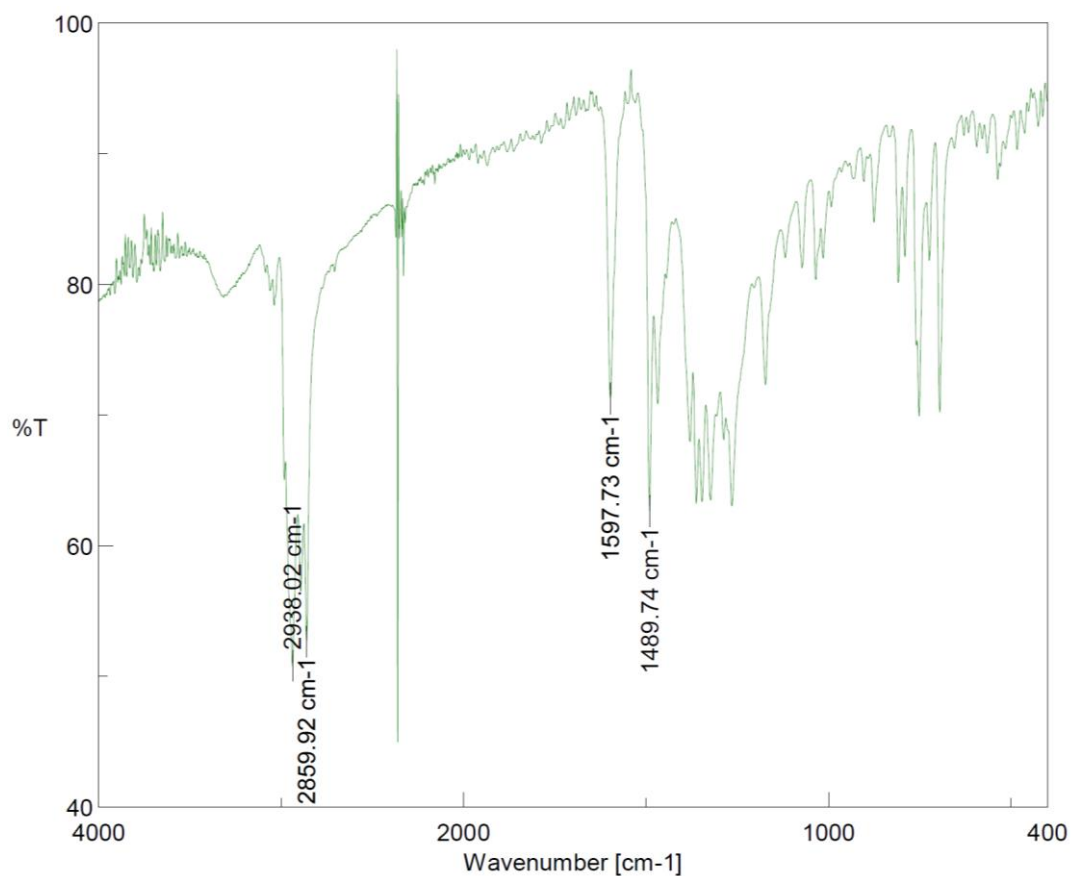


Figure S40. IR spectrum (ATR) for compound 5.

Mixture of 6a and 6b

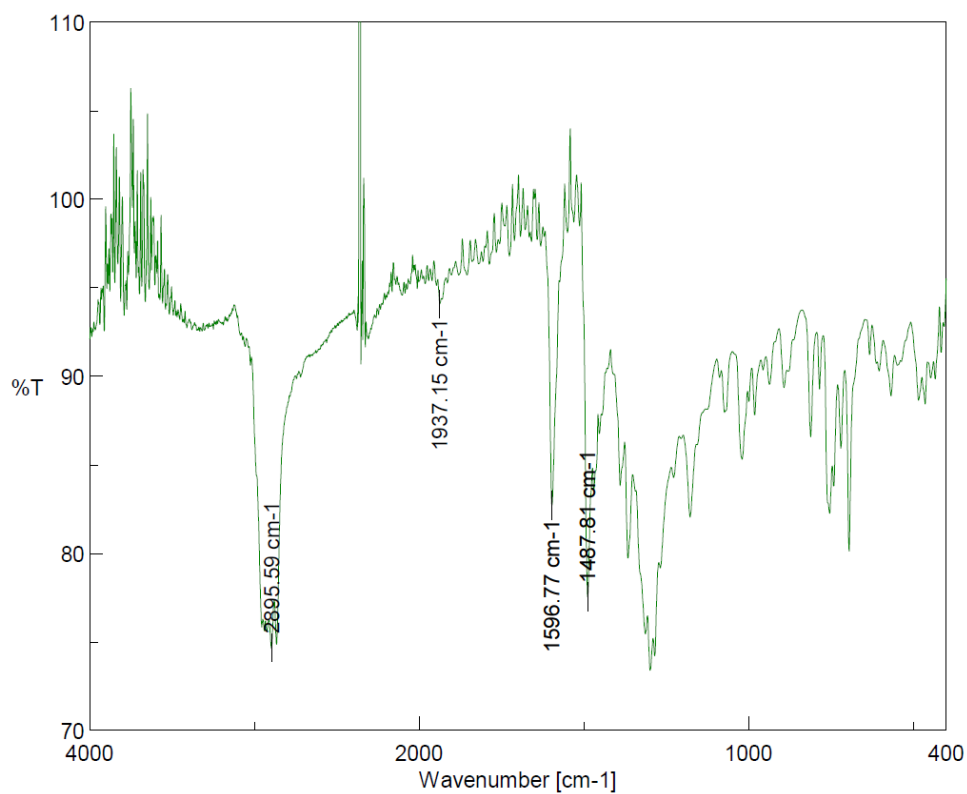


Figure S41. IR spectrum (ATR) for mixture of 6a and 6b (5:1).

Compound 7

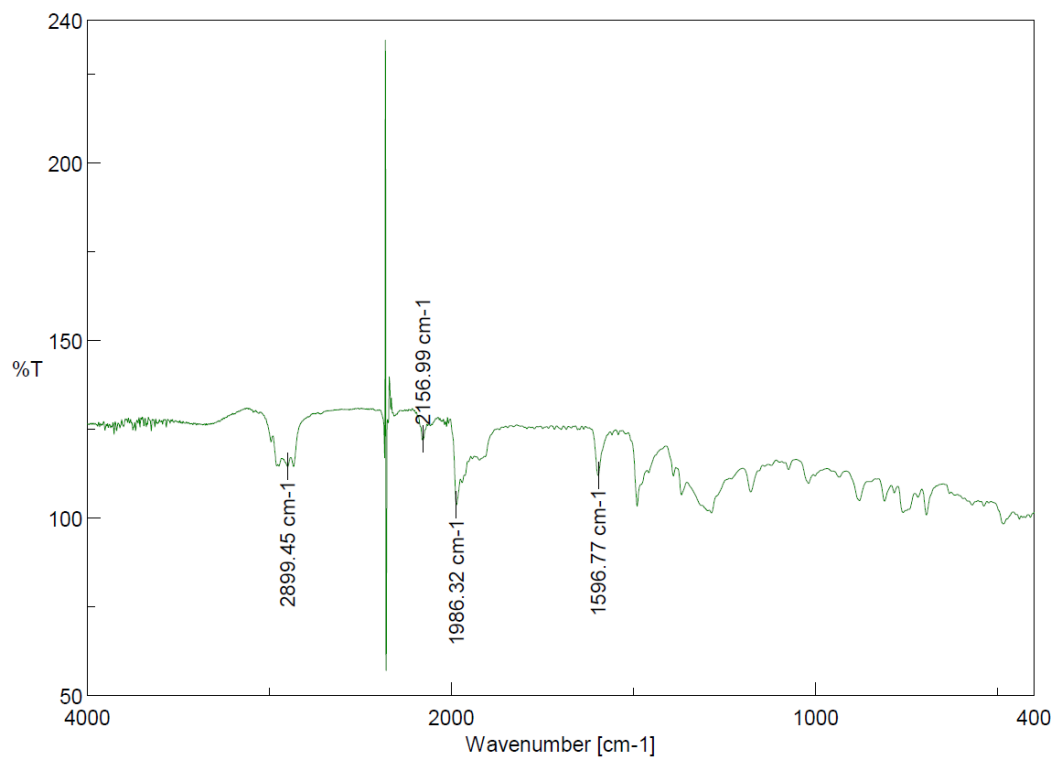


Figure S42. IR spectrum (ATR) for compound 7.

Compound 8

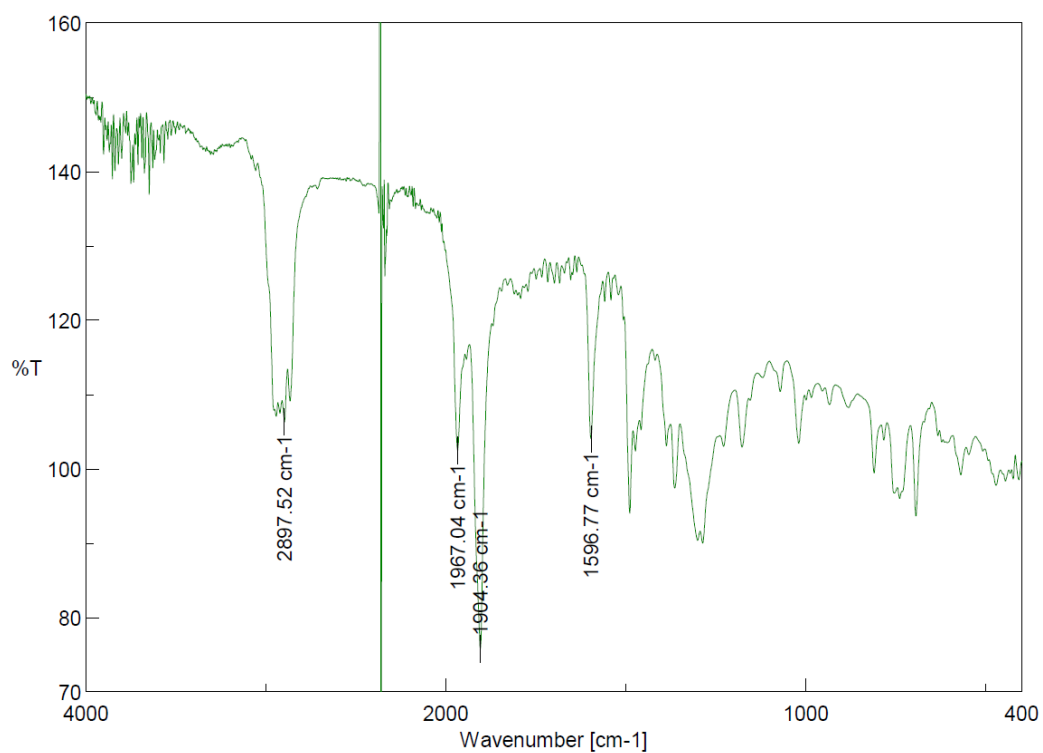


Figure S43. IR spectrum (ATR) for compound 8.

Compound 9

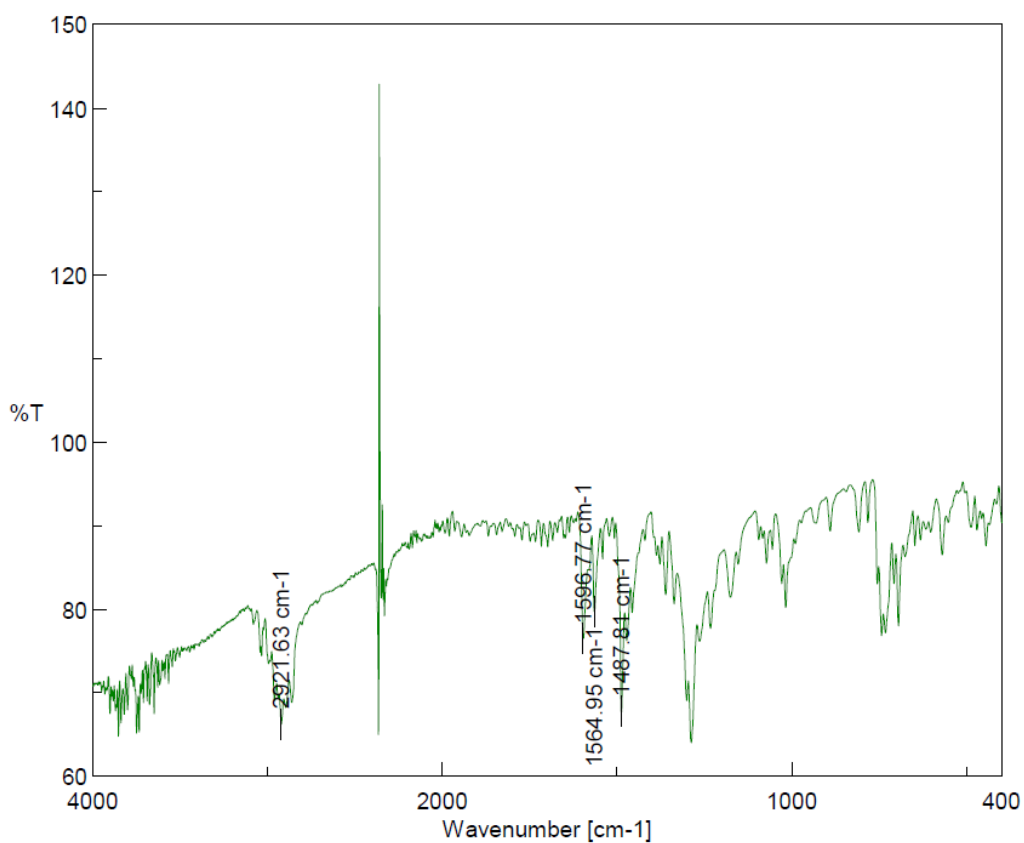


Figure S44. IR spectrum (ATR) for compound 9.

Compound 9_b

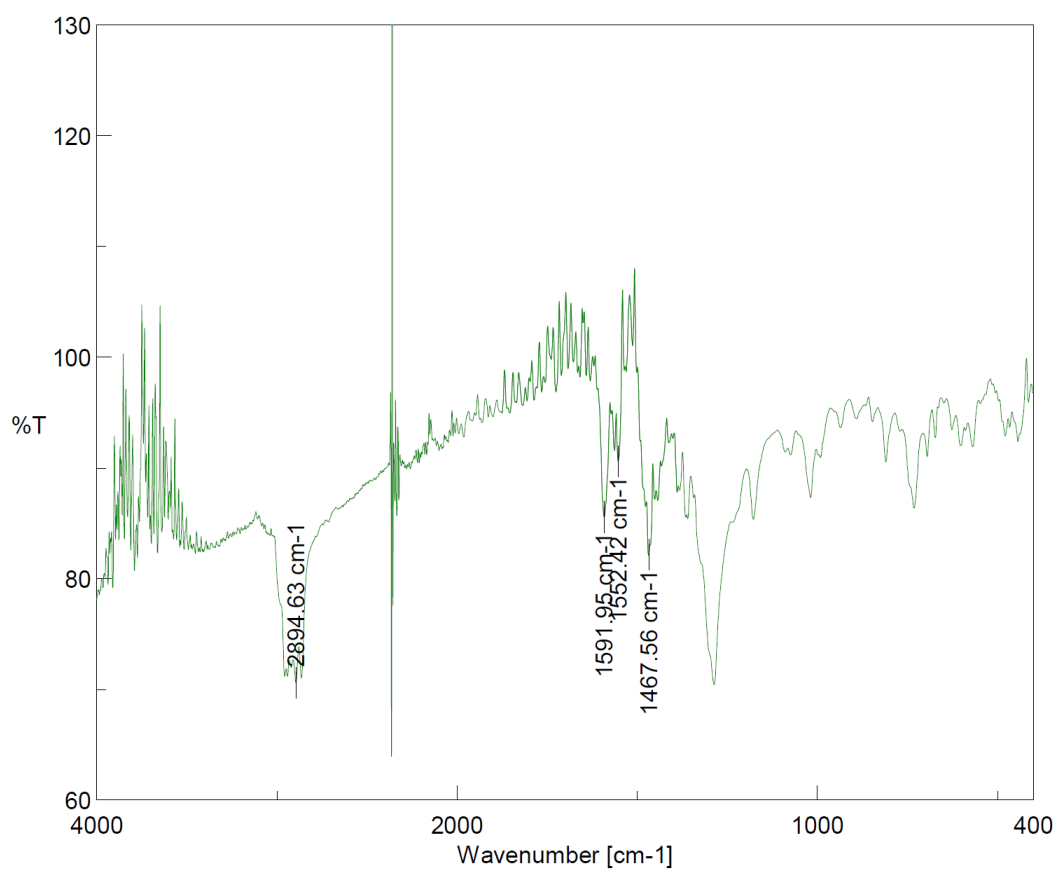


Figure S45. IR spectrum (ATR) for compound 9_b.

III. Detail for the X-ray Crystallographic Analyses

III-I. Instrumentation

X-ray crystallographic analyses of single crystals were performed on a Rigaku VariMax with Saturn diffractometer. A single crystal was mounted with mineral oil on a loop-type mount and transferred to the goniometer. The radiation was performed with graphite-monochromated Mo K α ($\lambda = 0.71075 \text{ \AA}$) at 50 kV and 24 mA. The structures were solved by the direct method with (SHELXT 2014) and refined by full-matrix least-squares techniques against F^2 (SHELXL 2014). The intensities were corrected for Lorentz and polarization effects. The nonhydrogen atoms were refined anisotropically.

III-II. Data for Compounds 4 and 5, Complexes 6b, 7, 8 and 9

III-II-I ORTEP Drawing for the Compound 4

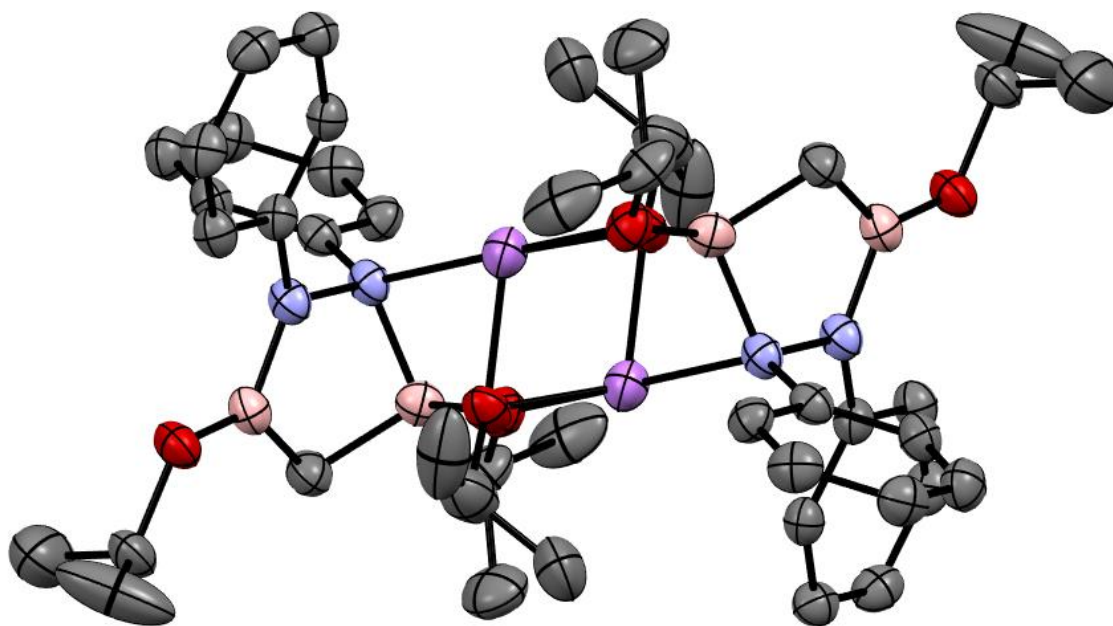


Figure S46. X-ray structure of **4**. (thermal ellipsoids are drawn with 50 % probability; hydrogen atoms on carbon atoms are omitted for clarity)

Table S2. Crystal data and structure refinement for **4** and **5**.

	4	5
CCDC number	2121282	2121283
Empirical formula	C ₂₂ H ₃₃ B ₂ LiN ₂ O ₃	C ₃₁ H ₅₂ B ₂ N ₂ P ₂

Formula weight		402.06	532.27
Temperature (K)		93	93
Wavelength (Å)		0.71073	0.71075
Crystal system		monoclinic	triclinic
Space group		$P2_1/c$	$P\bar{1}$
Unit cell dimensions	a (Å)	10.3563(8)	11.163(6)
	b (Å)	21.8893(14)	12.733(7)
	c (Å)	10.3352(8)	14.239(8)
	α (°)	90	102.894(2)
	β (°)	101.339(7)	106.128(6)
	γ (°)	90	112.723(5)
Volume (Å ³)		2308.3(3)	1664.0(16)
Z		4	2
Density (calculated) (g/m ³)		1.157	1.062
Absorption coefficient (mm ⁻¹)		0.074	0.151
$F(000)$		864	576
Theta (max)		28.886	24.998
Index ranges		$-13 \leq h \leq 13$	$-11 \leq h \leq 13$
		$-29 \leq k \leq 29$	$-15 \leq k \leq 15$
		$-11 \leq l \leq 13$	$-16 \leq l \leq 15$
Reflections collected		33618	11025
Independent reflections [R(int)]		5583 [R(int) = 0.1452]	5716 [R(int) = 0.0719]
Data Completeness (%)		0.922	0.977
Absorption correction		5583	5716
Refinement method		Multi-scan	Multi-scan
Data / restraints / parameters		5583 / 0 / 277	5716 / 0 / 346
Goodness-of-fit on F^2		1.038	1.045
Final R indices [$I > 2\sigma(I)$]		$R_1 = 0.1644$, $wR_2 = 0.3323$	$R_1 = 0.1193$, $wR_2 = 0.1698$
R indices (all data)		$R_1 = 0.1169$, $wR_2 = 0.3008$	$R_1 = 0.0737$, $wR_2 = 0.1401$
Largest diff. peak and hole (e.Å ⁻³)		1.365 / -0.409	0.348 / -0.366

Table S3. Crystal data and structure refinement for **6b** and **7**.

	6b	7
CCDC number	2121284	2121285
Empirical formula	$C_{31}H_{52}B_2ClIrN_2P_2$	$C_{32}H_{52}B_2ClIrN_2OP_2$
Formula weight	763.95	791.96
Temperature (K)	93	93
Wavelength (Å)	0.71073	0.71073
Crystal system	monoclinic	monoclinic
Space group	$P2_1/n$	$P2_1/n$

Unit cell dimensions	a (Å)	12.1553(3)	12.0281(3)
	b (Å)	18.4045(4)	19.0554(4)
	c (Å)	15.9578(4)	16.3403(4)
	α (°)	90	90
	β (°)	111.724(3)	111.042(3)
	γ (°)	90	90
Volume (Å ³)		3316.41(15)	3495.46(16)
Z		4	4
Density (calculated) (g/m ³)		1.530	1.505
Absorption coefficient (mm ⁻¹)		4.226	4.015
F(000)		1544	1600
Theta (max)		28.753	28.750
Index ranges		-16 ≤ h ≤ 15	-16 ≤ h ≤ 15
		-18 ≤ k ≤ 24	-22 ≤ k ≤ 25
		-20 ≤ l ≤ 21	-21 ≤ l ≤ 16
Reflections collected		28485	32953
Independent reflections [R(int)]		7754 [R(int) = 0.0318]	8159 [R(int) = 0.0289]
Data Completeness (%)		0.900	0.900
Absorption correction		7754	8159
Refinement method		Multi-scan	Multi-scan
Data / restraints / parameters		7754 / 0 / 368	8159 / 1 / 386
Goodness-of-fit on F ²		1.040	1.049
Final R indices [I > 2σ(I)]		R ₁ = 0.0255, wR ₂ = 0.0506	R ₁ = 0.0390, wR ₂ = 0.0903
R indices (all data)		R ₁ = 0.0209, wR ₂ = 0.0495	R ₁ = 0.0345, wR ₂ = 0.0883
Largest diff. peak and hole (e.Å ⁻³)		1.097 / -0.687	4.332 / -2.978

Table S4. Crystal data and structure refinement for **8** and **9**.

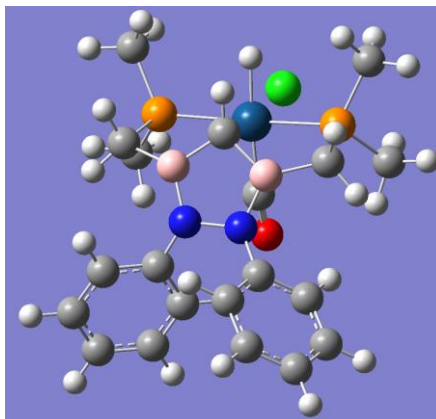
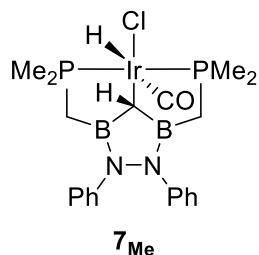
	8	9	
CCDC number	2121286	2121287	
Empirical formula	C ₃₂ H ₅₁ B ₂ IrN ₂ OP ₂	C ₃₇ H ₅₇ B ₂ IrN ₂ P ₂	
Formula weight	755.50	805.60	
Temperature (K)	93	93	
Wavelength (Å)	0.71073	0.71073	
Crystal system	monoclinic	monoclinic	
Space group	P ₂ ₁ /n	P ₂ ₁ /c	
Unit cell dimensions	a (Å)	12.1072(2)	12.0351(3)
	b (Å)	18.3581(3)	14.6757(4)
	c (Å)	16.2005(3)	20.6311(6)
	α (°)	90	90
	β (°)	111.723(2)	92.120(3)

	γ (°)	90	90
Volume (Å ³)		3345.09(11)	3641.44(17)
Z		4	4
Density (calculated) (g/m ³)		1.500	1.469
Absorption coefficient (mm ⁻¹)		4.114	3.782
F(000)		1528	1640
Theta (max)		28.632	25.000
Index ranges		-15 ≤ h ≤ 16	-14 ≤ h ≤ 14
		-24 ≤ k ≤ 24	-17 ≤ k ≤ 17
		-20 ≤ l ≤ 21	-23 ≤ l ≤ 24
Reflections collected		25796	30236
Independent reflections [R(int)]		7678 [R(int) = 0.0301]	6418 [R(int) = 0.0761]
Data Completeness (%)		0.895	0.999
Absorption correction		7678	6418
Refinement method		Multi-scan	Multi-scan
Data / restraints / parameters		7678 / 0 / 373	6418 / 6 / 414
Goodness-of-fit on F ²		1.036	1.097
Final R indices [$I > 2\sigma(I)$]		$R_1 = 0.0292$, $wR_2 = 0.0532$	$R_1 = 0.0397$, $wR_2 = 0.0976$
R indices (all data)		$R_1 = 0.0233$, $wR_2 = 0.0516$	$R_1 = 0.0371$, $wR_2 = 0.0964$
Largest diff. peak and hole (e.Å ⁻³)		1.271 / -0.981	3.339 / -2.716

IV. Methods and Discussions for Theoretical Calculations

DFT calculations were performed using the Gaussian 09 Program, revision C.01.⁶ All geometry optimizations followed by frequency calculations were performed using M06 functional and SDD basis set for iridium and 6-31G* basis set for other elements with SMD solvation model (benzene). NBO analyses were conducted with NBO 6.0. For calculations in section IV-III, Gaussian 16 program,⁷ M06 functional with Def2SVP basis sets were employed.

IV-I. NBO and MO Analysis of Complex **7_{Me}**

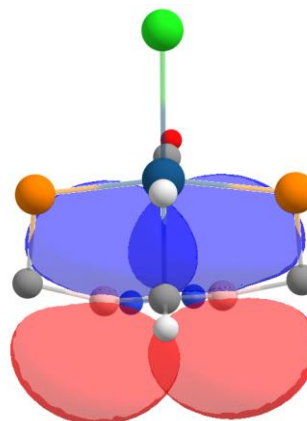
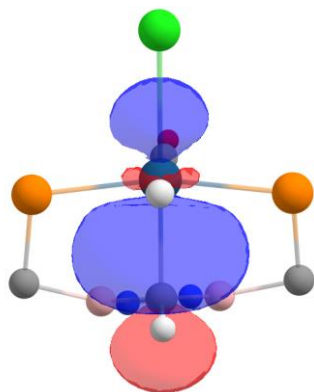


optimized structure of **7_{Me}**

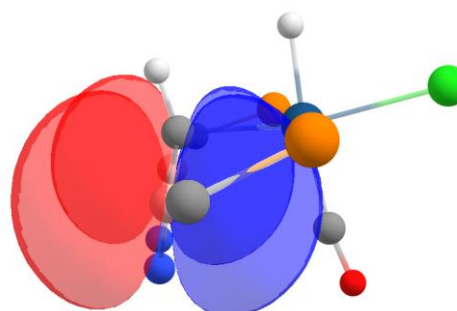
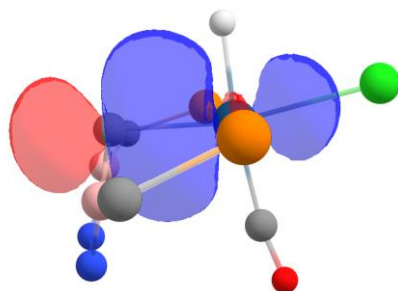
Ir-C bonding orbital

vacant p-orbitals of boron atoms

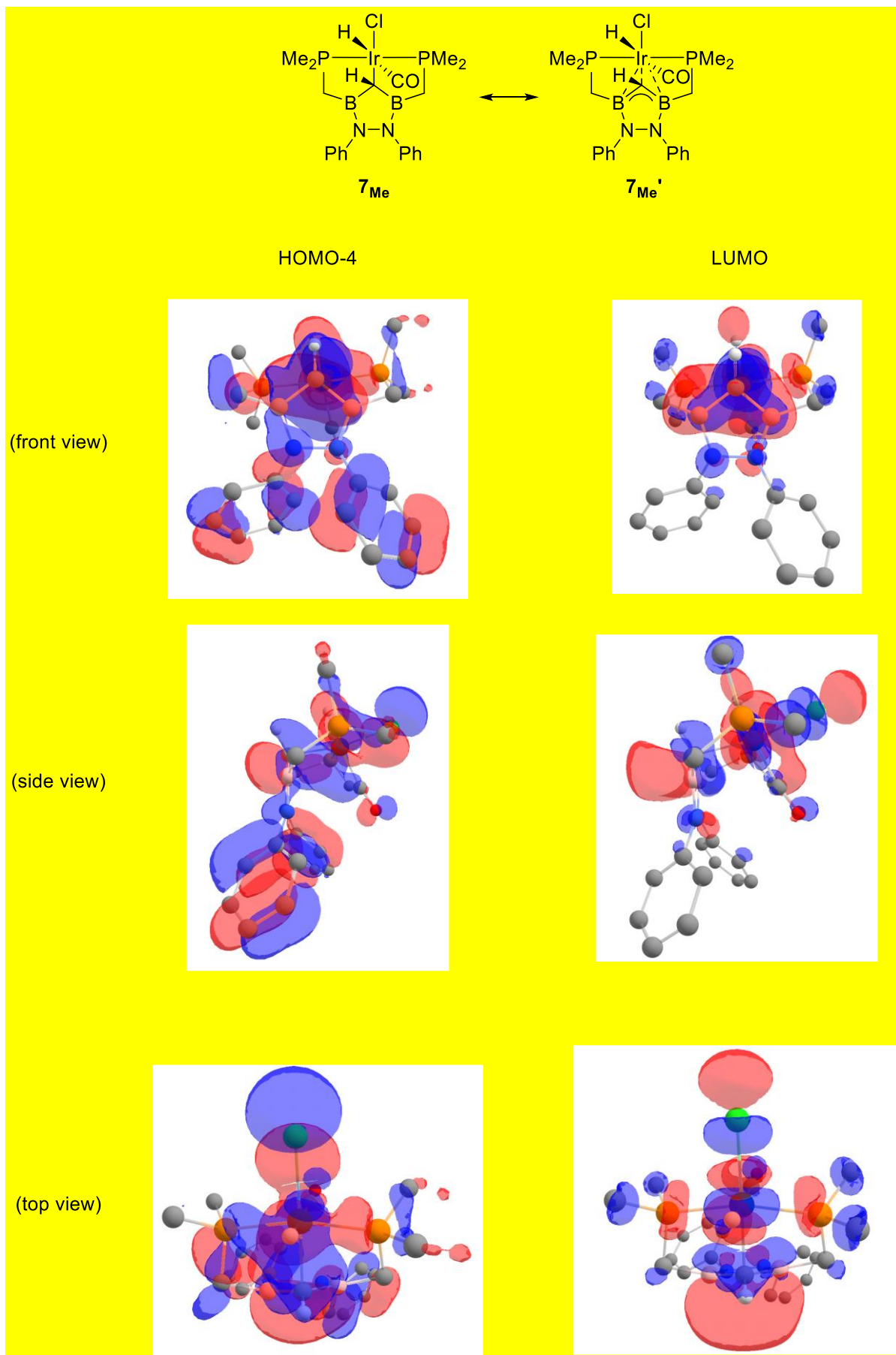
(top view)



(side view)

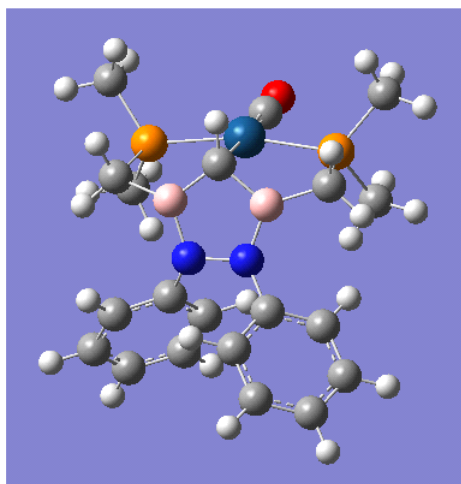
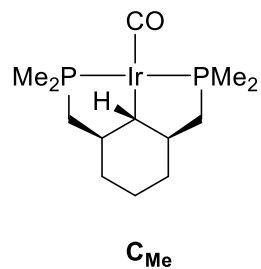
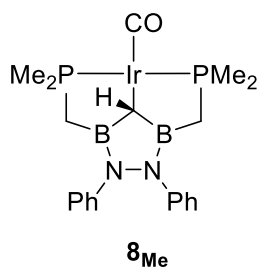


Total value of NBO second order perturbation from the Ir-C bonding orbital to the vacant p-orbitals of boron atoms was **344.77 kcal/mol**.

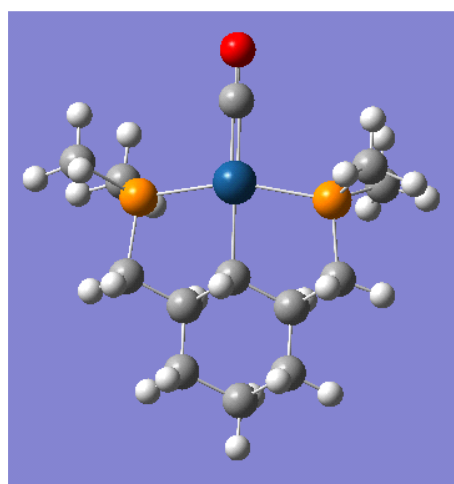


These two molecular orbitals support the contribution of $7_{Me'}$ in which the ligand CB_2N_2 ring takes η^3 -type coordination mode with carbon and boron atoms.

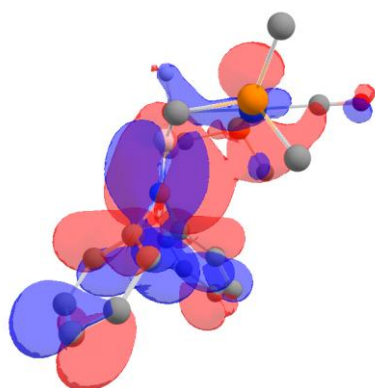
IV-II. Calculated Molecular Orbitals of Complexes $\mathbf{8_{Me}}$ and $\mathbf{C_{Me}}$



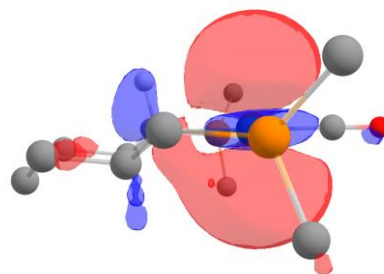
optimized structure of $\mathbf{8_{Me}}$



optimized structure of $\mathbf{C_{Me}}$



HOMO-1 of $\mathbf{8_{Me}}$

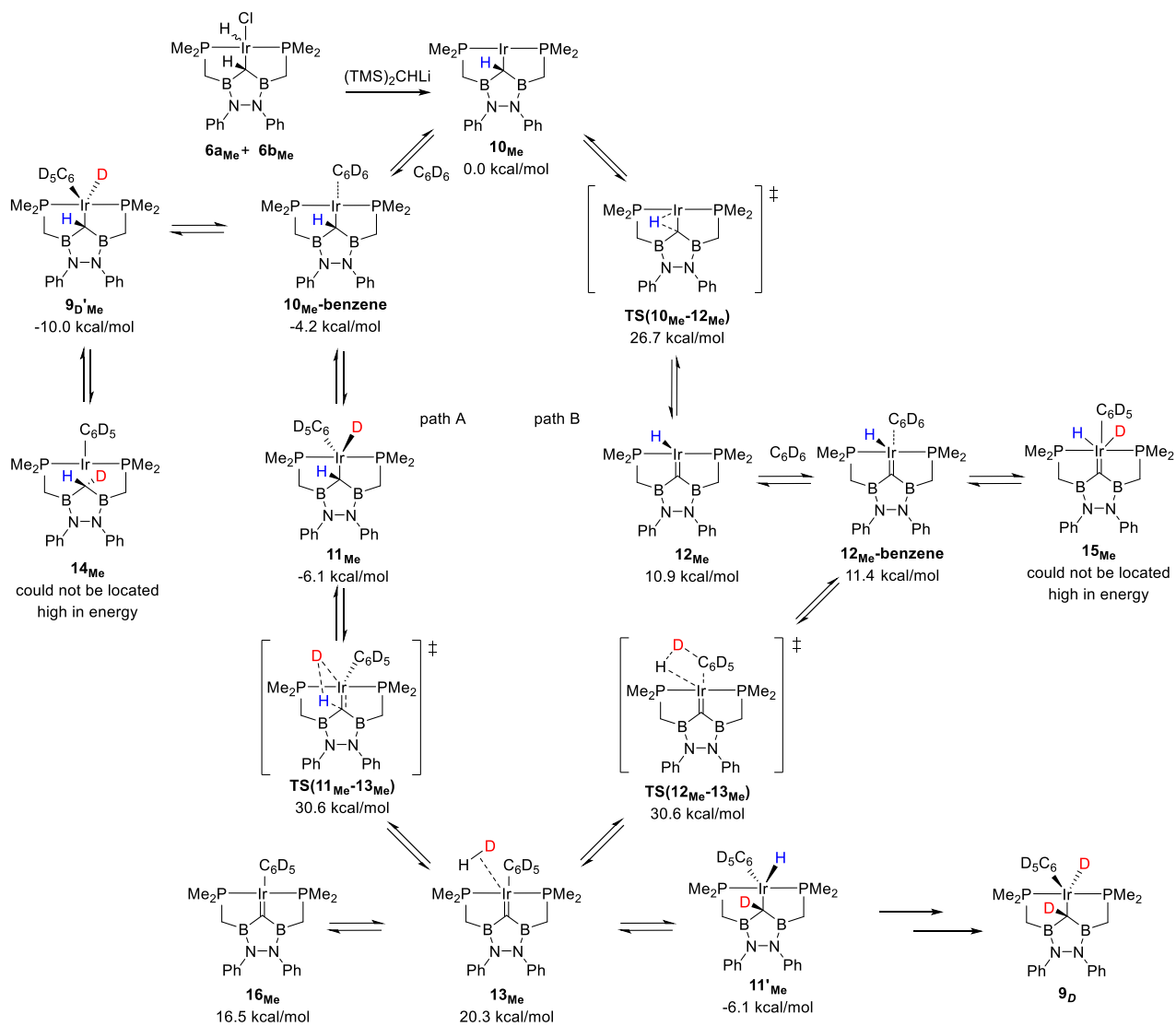


HOMO of $\mathbf{C_{Me}}$

In complex $\mathbf{8_{Me}}$, electrons in d_z^2 -orbital of Ir are delocalized to vacant orbitals on boron atoms (left). On the other hand, in the case of $\mathbf{C_{Me}}$, the electrons almost localize on the metal centre and partly α -carbon (right).

IV-III. Deuterium Incorporation at the α -Position

The possible reaction pathways for the deuterium incorporation at the α -carbon (Scheme 6 in the main text) were investigated by theoretical calculation with DFT (M06/Def2SVP, ^tBu groups on the phosphorous atoms were simplified to be methyl groups, ¹H was employed in place of ²H). The calculated structures and their free energy relative to complex **10**_{Me} are summarized in Scheme S4. It was found that the intermediacy of complex **14**_{Me} generated after C–H(D) bond reductive elimination from **9**_{D'}_{Me} is not feasible since we could not locate **14**_{Me} as a stable intermediate on calculation, which is in contrast to the reported mechanisms proposed with analogous PC(sp³)P-Ir complexes.⁸ Instead, there found a transition state (**TS(11**_{Me}**-13**_{Me}**)**) for hydrogen transfer from α -carbon to hydride (or deuteride) in complex **11**_{Me} which is the unstable isomer of **9**_{Me} formed after oxidative addition of C–D bond to complex **10**_{Me} (path A). The formation of phenyl diborylcarbene dihydrogen complex **13**_{Me} would allow the experimentally observed deuterium incorporation at the α -carbon with easy rotation of coordinating HD molecule. Another pathway (path B) is sigma-bond metathesis (**TS(12**_{Me}**-13**_{Me}**)**) of iridium-hydride bond in hydride diborylcarbene complex **12**_{Me} and C–D bond in coordinated benzene. The formation of analogous iridium hydride carbene intermediates (corresponding to **12**_{Me}) has been proposed in similar H/D exchange reactions with PCP-Ir complexes.^{8,9} In the precedented studies, oxidative addition of C–D bonds to Ir(I) carbene complexes was reported to be quite facile thus enable the H/D exchange at α -carbon. However, in our P_BC_BP system, the oxidative addition of C–D(C–H) bonds to **12**_{Me} was disfavored as the resulting Ir(III) complex **15**_{Me} could not be located as a stable intermediate in calculation and was seemingly too unstable to be considered. Thus as proposed in the main text (Scheme 6, path B), sigma-bond metathesis to afford phenyl carbene dihydrogen complex **13**_{Me} is proposed as a more plausible mechanism. It should be noted that, although paths A and B are the most feasible mechanisms among we investigated, the calculated absolute energy barriers are higher than expected as the H/D exchange reaction proceeded at room temperature.



Scheme S4. Entire proposed pathways (M06/Def2SVP level of theory). ^tBu groups were replaced with Me to simplify the calculation.

V. References

- [1] A. B. Pangborn, M. A. Giardello, R. H. Grubbs, R. K. Rosen and F. J. Timmers, *Organometallics*, 1996, **15**, 1518–1520.
- [2] H. A. Ali, I. Goldberg and M. Srebnik, *Organometallics*, 2001, **20**, 3962–3965.
- [3] C. N. Iverson, R. J. Lachicotte, C. Müller and W. D. Jones, *Organometallics*, 2002, **21**, 5320–5333.
- [4] A. van der Ent, A. L. Onderdelinden and R. A. Schunn, *Inorg. Synth.*, 1990, **28**, 91.
- [5] E. Le Coz, Z. Zhang, T. Roisnel, L. Cavallo, L. Falivene, J.-F. Carpentier and Y. Sarazin, *Chem. Eur. J.*, 2020, **26**, 3535–3544.
- [6] M.J. Frisch, G.W. Trucks, H.B. Schlegel, G.E. Scuseria, M.A. Robb, J. R. C.; G. Scalmani, V. Barone, B. Mennucci, G.A. Petersson, H. Nakatsuji, M. C.; X. Li, H.P. Hratchian, A.F. Izmaylov, J. Bloino, G. Zheng, J.L. Sonnenberg, M.; Hada, M. Ehara, K. Toyota, R. Fukuda, J. Hasegawa, M. Ishida, T. Nakajima, Y.; Honda, O. Kitao, H. Nakai, T. Vreven, J.J.A. Montgomery, J.E. Peralta, F. O.; M. Bearpark, J.J. Heyd, E. Brothers, K.N. Kudin, V.N. Staroverov, T. Keith, R.; Kobayashi, J. Normand, K. Raghavachari, A. Rendell, J.C. Burant, S.S. Iyengar, J.; Tomasi, M. Cossi, N. Rega, J.M. Millam, M. Klene, J.E. Knox, J.B. Cross, V. B.; C. Adamo, J. Jaramillo, R. Gomperts, R.E. Stratmann, O. Yazyev, A.J. Austin, R.; Cammi, C. Pomelli, J.W. Ochterski, R.L. Martin, K. Morokuma, V. G. Z.; G.A. Voth, P. Salvador, J.J. Dannenberg, S. Dapprich, A.D. Daniels, O. Farkas, J. B.; Foresman, J.V. Ortiz, J. Cioslowski, D. J. F. Gaussian 09 Revision E.01. 2010.
- [7] Frisch, M. J.; Trucks, G. W.; Schlegel, H. B.; Scuseria, G. E.; Robb, M. A.; Cheeseman, J. R.; Scalmani, G.; Barone, V.; Petersson, G. A.; Nakatsuji, H.; Li, X.; Caricato, M.; Marenich, A. V.; Bloino, J.; Janesko, B. G.; Gomperts, R.; Mennucci, B.; Hratchian, H. P.; Ortiz, J. V.; Izmaylov, A. F.; Sonnenberg, J. L.; Williams-Young, D.; Ding, F.; Lipparini, F.; Egidi, F.; Goings, J.; Peng, B.; Petrone, A.; Henderson, T.; Ranasinghe, D.; Zakrzewski, V. G.; Gao, J.; Rega, N.; Zheng, G.; Liang, W.; Hada, M.; Ehara, M.; Toyota, K.; Fukuda, R.; Hasegawa, J.; Ishida, M.; Nakajima, T.; Honda, Y.; Kitao, O.; Nakai, H.; Vreven, T.; Throssell, K.; Montgomery, Jr. J. A.; Peralta, J. E.; Ogliaro, F.; Bearpark, M. J.; Heyd, J. J.; Brothers, E. N.; Kudin, K. N.; Staroverov, V. N.; Keith, T. A.; Kobayashi, R.; Normand, J.; Raghavachari, K.; Rendell, A. P.; Burant, J. C.; Iyengar, S. S.; Tomasi, J.; Cossi, M.; Millam, J. M.; Klene, M.; Adamo, C.; Cammi, R.; Ochterski, J. W.; Martin, R. L.; Morokuma, K.; Farkas, O.; Foresman, J. B.; Fox, D. J. Gaussian 16, Revision C.01, Gaussian, Inc., Wallingford CT, 2016.
- [8] (a) J. Zhou and J. F. Hartwig, *Angew. Chem., Int. Ed.*, 2008, **47**, 5783–5787; (b) A. V. Polukeev, R. Marcos, M. S. G. Ahlquist and O. F. Wendt, *Organometallics*, 2016, **35**, 2600–2608.
- [9] J. D. Smith, G. Durrant, D. H. Ess, B. S. Gelfand, W. E. Piers, *Chem. Sci.* 2020, **11**, 10705–10717.